The Evolution of Intelligence and Civilization

How Thermodynamic Constraints

Shape Minds, Societies, and History

Helmuth Nyborg

Kasandrobooks 2026

ISBN 97887-975215-2-6 (paperback)

Acknowledgement: Language editing assistance was provided using ChatGPT (OpenAI), with all content reviewed and verified by the author.

ISBN 97887-975215-2-6 (paperback)

Epigraph

"Panta rhei" (πάντα ῥεῖ)

"Everything is in flux; stability is an illusion, and reality consists of continuous process and transformation" (Heraclitus, c. 2,566–2,506 Kya).

We take this pre-Socratic insight to imply that all biological and societal structures are transient configurations of energy flow, stabilized through selection under constraint and dissolved when those constraints shift.

According to our MESTR framework, selection operates on the efficiency and organization of energy throughput under fluctuating constraints, and all adaptations reflect continuous trade-offs.

Cognition, institutions, and civilization emerge as temporary thermodynamic stabilizations of continuous energetic throughput under constraint. Stability is therefore always dynamic stability, and identity is best understood as a time-averaged pattern.

Complexity arises as organization imposed on flow under constraint. Institutions are macroscopic solutions to energetic coordination problems, and human civilization represents not an exception to physical law, but its most complex expression in the domain of energy-coordinated systems.

PART I – Foundations

1. Introduction

Human evolution and societal development can be reframed as thermodynamic processes governed by energy flow, constraint, and allocation. Across latitudes, declining solar energy and increasing seasonality impose systematic constraints on survival, cooperation, and organization.

We test the hypothesis that long-run exposure to environmental harshness—captured by a composite Environmental Harshness Index (EHI)—structures genetic, morphological, cognitive, and institutional variation across Afro–European populations. Populations residing within ecozones are expected to undergo polygenic adaptation to local average constraint; this is evaluated using continuous EHI correlations and ecozone comparisons.

The Migration–Energy-Selection–Trait Redistribution (MESTR) framework integrates (i) a geo-temporal scaffold from haplogroups and ancient DNA, (ii) a composite EHI (photoperiod, thermal seasonality, winter length, irradiance), and (iii) biological, cognitive, life-history, and institutional data.

Intelligence is treated as a coordination-intensive, energy-constrained adaptation.

The monograph proceeds from EHI construction to continuous and ecozone analyses, where ecozones represent discretized segments of the continuous EHI gradient, followed by a discussion of implications and limitations within a thermodynamic framework.

1.2 MESTR: Migratory–Energetic Selection and Trade-offs

The Migration - Energetic - Selection and Trade-off framework (MESTR) models how organisms evolve under energetic constraint. Total migratory energy must be partitioned across competing functions:

$$E_{total} = E_{maint} + E_{growth} + E_{repro} + E_{neural} + E_{buffer}$$

When environmental harshness increases:

$$E_{maint}, E_{buffer} \uparrow \Rightarrow E_{growth}, E_{neural}, E_{repro} \downarrow$$

This produces systematic energetic trade-offs in life-history strategy and organismal design (Stearns, 1992; Kaplan et al., 2000).

Under higher energetic constraint:

- Maintenance dominates metabolism
- Storage and risk buffering increase
- Development slows
- Coordination and planning gain adaptive value

Under lower constraint:

- Energetic surplus increases
- Development becomes faster
- Neural investment decreases
- Complex behavioral and cooperative systems de-evolve

MESTR therefore interprets biological evolution as constrained optimization of metabolic allocation under variable energetic boundary conditions.

1.3 Energetic surplus and neural investment

Neural tissue is metabolically expensive and requires stable energetic surplus (Aiello & Wheeler, 1995; Kuzawa et al., 2014).

The EHI–MESTR framework predicts:

$$E_{neural} \propto E_{surplus}$$

Stable surplus permits:

- Extended juvenile development
- Greater neural coordination
- Long-horizon planning and storage
- Complex social organization

Where energetic constraint dominates, metabolic economy and survival efficiency are favored instead.

1.4 Testable Predictions of the EHI–MESTR Framework

The framework generates explicit, falsifiable predictions:

1.4.1 Energetic Constraint Gradient

$$EHI \uparrow \Rightarrow E_{surplus} \downarrow$$

Observable as decreasing ecological productivity relative to survival cost.

1.4.2 Life-history Trade-offs

Higher EHI environments predict:

- Slower development
- Greater buffering/storage behavior
- Increased coordination demand (Stearns, 1992)

1.4.3 Neural Investment Relationship

Stable surplus environments should correlate with greater neural metabolic allocation (Pontzer, 2017).

1.4.4 Seasonality and Planning

Greater photoperiod variability predicts stronger anticipatory and storage strategies.

1.4.5 Energetic Stability Hypothesis

Systems under high constraint should prioritize variance reduction over throughput maximization (Odum, 1995).

1.4.6 Macro-ecological Gradient

EHI should correlate with:

- Productivity
- Climatic variability
- Seasonal energy accessibility

These predictions are empirically testable using ecological, physiological, and macro-scale environmental datasets.

1.5 Thermodynamic constraint formalization

The EHI quantifies the net energetic burden imposed by the environment. It represents the relationship between usable ecological energy and the metabolic cost required for survival and stability.

Let:

E_{in} = metabolically usable environmental energy

E_{maint} = baseline survival and maintenance cost

$E_{surplus}$= energy available for growth, neural investment, and buffering

$$E_{surplus} = E_{in} - E_{maint}$$

Environmental harshness can be interpreted as the relative constraint on surplus:

$$EHI \propto \frac{E_{maint}}{E_{in}}$$

where:

the empirical EHI is an operational proxy for the theoretical ratio E_{maint}/E_{in}.

High EHI corresponds to high constraint and reduced surplus; low EHI corresponds to greater available surplus energy. This formulation reflects a fundamental ecological principle: organismal strategy depends not on absolute energy input alone, but on net usable surplus after survival costs are met (Brown et al., 2004; Pontzer, 2017).

1.6 MESTR Energetics

MESTR posits that migration alters the energetic environment faced by populations, leading to directional selection on genes for traits that improve energy acquisition, buffering, and allocation. Harsh environments magnify the fitness consequences of inefficiency. Traits that reduce waste, improve planning, and enhance coordination are therefore increasingly favored as ecological margins narrow.

In energetic terms, genetically more homogeneous populations exhibit lower coordination costs. This matters under MESTR because in energetically harsh environments, inefficiencies in cooperation, trust, and division of labor are more costly, so selection therefore favors population structures in which relatedness and similarity reduce friction in social coordination.

1.7 Geotemporal scaffold from Y-haplogroups

We use Y-chromosome and mitochondrial haplogroups to construct a chronological, geo-temporal scaffold for MESTR.

Table 1. Geo-temporal scaffold for MESTR (Author-generated schematics).

Evolutionary timetable	Generations	Haplogroup Male	Haplogroup Female	Direction	Ecotype, place, and action
2018	1	R1b			1. Denmark. R1b is the dominant y-Haplotype frequency in the core polygon area (Murray, 2003) of north-western Europe.
-1.300	52				Northern Italy. This haplotype is observed in numbers in the Partecipanza population in San Giovanni, near Bologna, Northern Italy, in a time of heavy political turmoil and migratory activity.
-3.000	120	I-L22			
-12.000 - -15.000	600 - 480	I-M253			1. Europeans returning up North again after the retreat of glaciers, and their y-Haplotype group is most common today in Denmark, southern Sweden, and Norway (38%-31.5%).
-18.000 - -28.000	1.120 - 720				1. Ice Age in Europe. Southern retreat. The advancing Ice Age glaciers pushes European inhabitants back out of interior Europe and into its southern fringes like Iberia, the Italian peninsula, the Balkans (and perhaps even down to northern Africa to rule classical Egypt?).
-30.000 - -45.000	1.920	I-M170			2. Southern Europe. First to invade Europe. Largely seen today only in Europe (≈20%) Scandinavia (≈45%). Forming Gravettian culture; moving southeast to northwest across the continent; split 30.000 years ago when some migrated further up north across the continent, introducing new stone tool technology and art forms like the "Venus" figurine. Going North.
-59.000	2.360	N			African exodus.
-65.000	2.600			L3	3. North Africa. Going North,
-76.000	3.040	F-M89			4. Central Africa. Going North.
-275.000	11.000	I-L25.1			5. Equatorial Africa. Going North.

The scaffold (Table 1) does two things:

- it confirms an equatorial origin for anatomically modern humans; and
- it sketches a latitudinal migration timetable.

Each row in the scaffold corresponds to an approximate date (in thousands of years ago), an estimated number of generations, representative Y-haplogroups and mitochondrial lineages, and a narrative waypoint along the inferred migration trajectory.

The haplogroup waypoints are based on analysis of the author's 23andMe assay (2019). That lineage exits tropical Africa, moves through Central and North Africa, crosses into southern Europe, and eventually reaches northern Europe. This path mirrors well-known "out-of-Africa" dispersal corridors and later post-glacial recolonizations.

Competition for increasingly scarce energy resources serves as the primary selective principle in MESTR, favoring genotypes and phenotypes that can capture, manage, and allocate energy more efficiently under high EHI conditions. Prehistoric latitudinal migration under varying EHI conditions enables us to examine two related aspects of our basic energetic hypothesis:

Migrants who finally settled in the northern European ecozone had gradually adapted to the highest levels of EHI.

Many migrants established permanent residency within one of the remaining four ecozones short of the northernmost ecozone, developed polygenic adaptations over multiple generations to the local average EHI, and slowly approached local equilibrium under sustained selection.

Environmental harshness systematically constrains admissible variance in coordination-relevant traits through energetic selection and truncation dynamics.

Key stages include:

A Late Pleistocene exodus from Africa (~59–45 Kya), with a founder effect/bottleneck and reduced genetic diversity relative to contemporary sub-Saharan populations.

Post-glacial recolonization of northern Europe by lineages such as I-M253 and I-L22.

Bronze-Age steppe incursions (Yamnaya and related groups) from the Pontic-Caspian steppe into northwestern Europe.

The contemporary frequency of I1 in Denmark, southern Sweden, and Norway (~31–38%) and the dominance of R1b in northwestern Europe are consistent with this northern scaffold. The ancestral path can be summarized (for descriptive purposes) as: Near Equatorial Africa (Ecozone 5) → Subtropical/Sahel Africa (Ecozone 4) → North Africa/Magreb (Ecozone 3) → Southern Europe (Ecozone 2) → Northern Europe (Ecozone 1).

1.8 Northern European transitions

Two northern transitions are especially relevant for MESTR:

1.8.1 Post-glacial recolonization

I-L22 and I-M253 lineages rise in frequency in Scandinavia and adjacent regions after ice retreat, consistent with recolonization from southern refugia. I1 today remains common in Denmark, southern Sweden, and Norway.

1.8.2 Steppe expansions

Beginning ~5.5–4.5 Kya, Yamnaya-derived groups moved westward from highly seasonal steppe ecologies north of the Black Sea (Anthony, 2007; Lazaridis et al., 2025). This movement reshaped paternal line pools across northwestern Europe and appears to reflect selection under extreme seasonal temperature swings in continental interiors.

1.9 Environmental drivers and transformations

The MESTR structure is:

Independent driver:

Solar irradiation (W m^{-2}), used as a proxy for available energy to ecosystems and human societies.

Redistribution of metabolic investment across genes, endocrine factors, neural tissue, and organ systems (behavioral/physiological adaptation).

1.10 EHI

The Environmental Harshness Index (EHI) operationalizes thermodynamic constraint as the environmental boundary condition under which biological and societal systems evolve. It combines standardized measures of (i) winter length, (ii) photoperiod variability, (iii) temperature seasonality, and (iv) solar irradiance (inverted). Higher values indicate greater constraint.

Components are z-scored and averaged; a PCA-weighted variant (rescaled 0–100) yields near-identical rankings ($r \approx .98$). EHI therefore captures the meridional gradient in energy availability and seasonal constraint.

1.11 Energetic selection by ecozone

To summarize large-scale environmental gradients, we grouped countries into latitude-defined ecozones. Absolute latitude (capital latitude in degrees north, ignoring sign for southern latitudes) was partitioned into:

Three equal-width bands from 0°N to 37°N for Africa.

Two equal-width bands from 37°N to 71°N for Europe.

For each band we calculated the number of countries (n) and the mean EHI, within-band standard deviation (SD), and the standard error of the mean (SEM).

Table 2. EHI by latitude-defined ecozone

Ecozone	Capital Latitude range (°N)	N	EHI PCA (0-100)	SD	SEM
Europe 1: Northern	48.40 – 64.00	17	85.11	7.36	1.79
Europe 2: Southern	34.00 – 47.20	15	65.10	7.69	1.98
Africa 3: Northern/ Maghreb	25.00 – 32.00	7	38.13	4.40	1.66
Africa 4: Subtropical / Sahel	12.00 – 22.00	17	17.22	4.86	1.18
Africa 5: Near-Equatorial	1.00 – 11.30	22	7.80	3.37	0.72

Note. Latitude ranges are absolute (capital) latitudes in degrees north.

Higher EHI pca weighted values (rescaled 0-100) indicate more energetically and climatically harsh environments (longer/darker winters, stronger photoperiod deficits, greater seasonal thermal amplitude, and lower 1997–2003 irradiance in W m^{-2}).

As expected, EHI is highest in the most poleward ecozone (54–71°N) and decreases stepwise toward the equator, with near-equatorial Africa (1–11.3°N) showing the lowest mean EHI. This latitudinal gradient reflects systematically longer winters, deeper photoperiod deficits, and stronger thermal seasonality at higher latitudes.

1.12 The MESTR Framework

Figure 1. Schematic representation of the MESTR framework (Author-generated schematics).

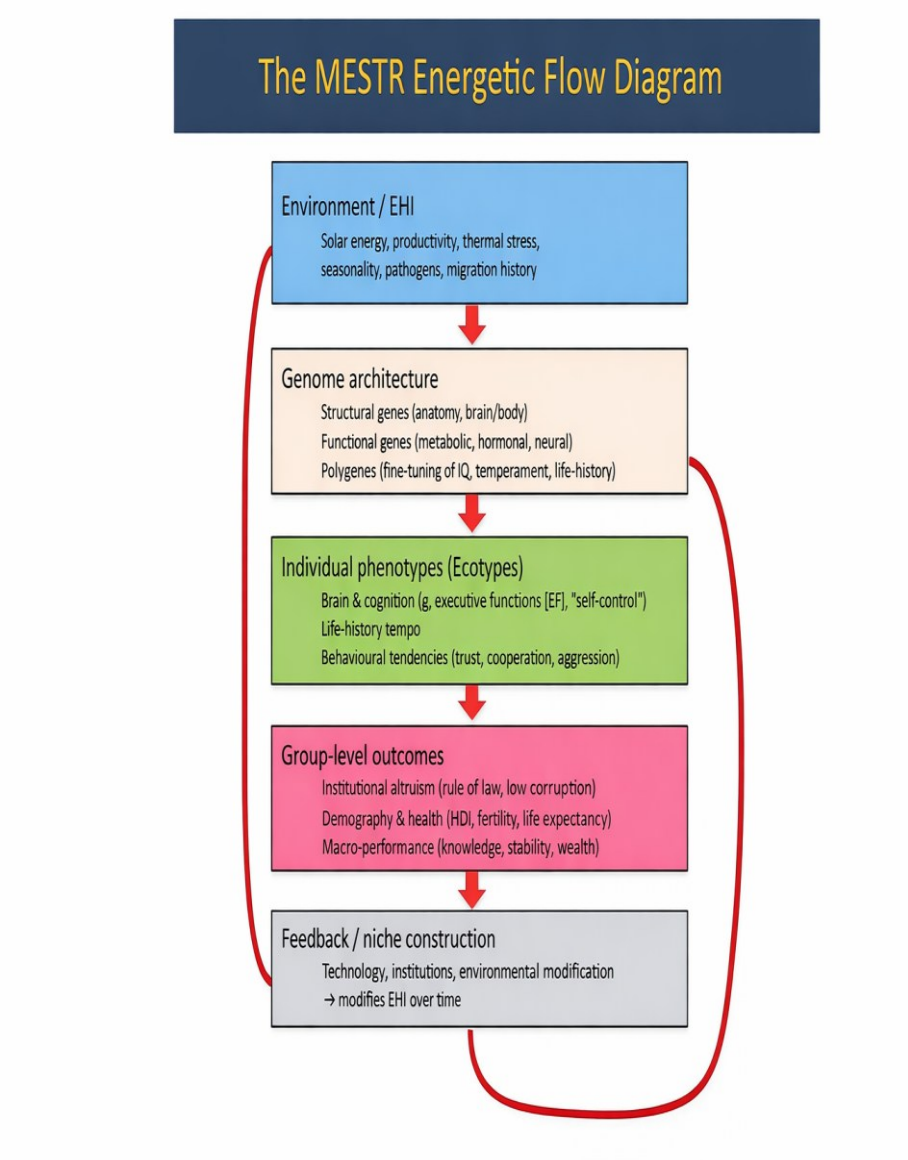

The figure represents a simplified MESTR architecture. Eco-harshness (EHI) in different environments shapes selection on genome architecture (structural, functional, and polygenic variants, see below), which builds individual phenotypes (brains and cognition, life-history strategies, behavioral tendencies). These, in turn, generate group-level outcomes (institutional altruism, demography, knowledge production, stability, wealth), which feed-back via niche construction to modify the energy–harshness regime over time.

1.13 Gene circuit designs

1.13.1 Structural genes.

Structural genes store information in DNA, while the actual energy resides in ATP, ion gradients, heat, mechanical work, and other forms of energetic activity. They build the organism's basic morphology—body and brain size, skull shape, vasculature, insulation, and so forth—and thereby define a baseline morphological "wiring diagram" for energy flow. In the MESTR framework, structural genes render an organism eligible to operate in a given EHI regime (for example, large brains with adequate thermoregulation in harsh ecozones). Metaphorically, they are analogous to the printed circuit board and components in an engineered system.

1.13.2 Functional genes.

Functional genes code for enzymes, ion channels, receptors, hormones, and regulatory factors. They provide the rules by which energy is allocated moment-to-moment: whether to increase or conserve metabolic output, whether to invest in offspring quantity versus quality, and whether to maintain high prefrontal activity under stress or flip into limbic emergency modes. In the MESTR perspective, functional genes implement the dynamic control

systems that channel energy through the structures specified by structural genes.

1.13.3 Polygenes.

Most traits of interest in MESTR—intelligence, height, life-history tempo, altruism, and many societally relevant behaviors—are highly polygenic. Each locus has only a tiny effect, but in aggregate, thousands of variants fine-tune how much brain tissue is grown, how efficiently it is run, and key behavioral tendencies such as risk-taking, long-term planning, and social trust. Under sustained EHI, selection does not act on a single large "intelligence gene" but instead nudges allele frequencies at many loci, gradually tuning the entire thermodynamic–behavioral circuit. Polygenic variation thus functions like thousands of small adjustment knobs distributed across the system.

1.13.4 Structured cascade

In other words, EHI is like the external load and supply conditions; selection favors genomes whose "circuit designs" transform that incoming energy into survival, brainwork, and cooperation more efficiently than rival designs; and EHI slowly nudges allele frequencies of thousands of variant polygenes that slightly lower or raise energy costs, improve information processing per unit energy, and improve coordination and cooperation in that ecozone.

The MESTR framework implies a structured cascade as formalized in Part III.

The following section details the empirical construction of variables, data sources, and statistical procedures used to test the MESTR framework.

PART II – Methods

EHI was constructed as a composite of winter length, photoperiod variability, temperature seasonality, and irradiance (inverted), standardized and averaged. EHI represents thermodynamic (energetic) constraint. Unless otherwise stated, EHI refers to the PCA-weighted 0–100 version. Full specification is provided in Appendix A.

2.1 Study domain and geographic mask

To maximize the interpretable north–south (meridional) migration and exposure signal — and to limit confounding from longer Eurasian resettlements, some associated with repeated glacial advances and retreats — analyses are restricted to:

Africa: 48 mainland countries (excluding small islands with historically easy maritime access).

Europe: 30 countries.

Longitude window: 15°W to 30°E (−15…+30).

Latitude range: 0°N to 71°N for most analyses.

These spatial masks are the same windows later used for environmental, genetic, and socioeconomic aggregation.

2.2 Data handling and quality control

All environmental variables were land-masked and aggregated to the country polygon intersecting the study window.

When combining sources with different vintages, we used the closest long-term climatological baselines and documented any rank inversions.

Units were standardized: °C, W m^{-2}, cm^3. European decimals (e.g., 275.000) were converted to English style (275,000) in text and tables.

Sensitivity checks included repeating analyses with population-weighted aggregations and alternative thresholds for the longitude mask.

2.3 Genetic, anthropometric, educational, and societal covariates

Contemporary genetic distance (male line): Mean of five distance metrics (Rogers, Prevosti, Cavalli-Sforza & Edwards chord, Nei, etc.) computed from Y-haplogroup frequencies across the following sets: BT, B, C, DE, D, E, F, G, H, I, J, K, L, NO, N, O, P, Q, R, T by Rindermann & Becker (2016).

Haplogroup frequency datasets: HGSP/HGSN counts from Rindermann, Woodley, & Stratford (2012); raw files obtained via Cherson (2012) and updated by Rindermann & Becker (2016).

Historic genetic Distance, F_{ST} or co-ancestor coefficients, measuring genealogical distance between ancient populations. As Cavalli-Sforza et al. (1994, pp. 75–76) emphasize, the major gradients in genetic variation across Eurasia closely follow the main axes of prehistoric migration, with a pronounced cline running from the Near East into Europe. (original data from Cavalli-Sforza et al., 1994), matched from populations to countries by Spolaore and Wacziarg (2006).

Paleo-cranial capacity (cm^3): Beals, Smith & Dodd's (1984) compilation (n = 122 pre-colonial samples, 1.2 Mya–10 Kya) geo-linked to modern borders via Becker (2019).

Average skin color of population in pre-colonial times, from Biasutti (1967, Pigmentation map, Fig. 6), range 1-8, reverse-coded so that lower scores indicate lighter native skin pigmentation, number of skin color gradients weighted by estimated population proportions, and overlaid to map of the world with current borderlines.

Body height (means) 1896–1996 (cm) (NCD Risk Factor Collaboration, 2016).

Mean BMI in adults 1975–2016 (NCD Risk Factor Collaboration, 2017).

Body weight (means) calculated from body height and BMI.

CAG repeats (Ellis et al., 2021). A three-base DNA motif of cytosine-adenine-guanine repeated differentially 8-35 times in exon 1 of the androgen receptor (AR).

National cognitive/related indices: Jensen & Kirkegaard (2024).

Student assessment IQ (SASIQ, PISAIQ, TIMSSIQ, PIRLSIQ results (Rindermann, 2007, 2018; Lim et al., 2018).

Expected years of schooling (2023), projected years of schooling for a child of school entrance age if current age-specific enrolment rates persist, from the UNDP Human Development Report statistical database (UNDP, 2024).

Education Index (2023), HDI education component based on the equally weighted indices of mean years of schooling (adults 25+) and expected years of schooling (children of school-entry age), from the UNDP Human

Development Data Center, HDR 2025 Statistical Annex, Table 1 “Human Development Index and its components” (UNDP, 2024).

Mother’s mean age at first birth (2006–2015), country estimates (years) from the CIA World Factbook field “Mother’s mean age at first birth”, using the latest available value in the 2006–2015 window for each country (Central Intelligence Agency, 2022).

Governance and development covariates:

Institutional altruism = first PCA component of Access to Basic Knowledge, Personal Freedom and Choice, Foundations of Wellbeing, Tolerance and Inclusion, Community Safety Net (0–100), Social Progress Index, Basic Human Needs, and Opportunity (higher = more supportive institutions).

Scientific & Technical Journal Articles per 1,000 people (2017), number of scientific and technical journal articles per 1,000 population in 2017, from the World Bank World Development Indicators series based on National Science Foundation / SCImago data (World Bank, 2024a).

Achievement: G. Meisenberg (Intelligence, 2015).

Income Index (2023), derived from GNI per capita in PPP terms within the UNDP Human Development Index framework (UNDP, 2024).

Life Expectancy Index (2023): HDI health component based on life expectancy at birth, from UNDP Human Development Data Center, HDR 2025 Statistical Annex, Table 1 “Human Development Index and its components” (UNDP, 2024).

Human Development Index, HDI 2023 (geometric mean of health, education, and income indices; UNDP, 2024).

Democracy Rank Index 2023 (The Economist Intelligence Unit: Age of conflict, 2024). London, UK. Democracy (higher = more democratic).

United Nations Development Programme. (2022). Human Development Report 2021/2022: Uncertain times, unsettled lives: Shaping our future in a transforming world. New York, NY: UNDP.

Gini coefficient (World Bank estimate, 2017; World Bank, 2024b).

Global Happiness (2015), average national life evaluation scores from the World Happiness Report 2015 (Helliwell, Layard, & Sachs, 2015).

Ethnic heterogeneity (EH) is calculated as the arithmetic mean of the inverse percentages of the three largest racial/ethnic, linguistic, and religious groups in each country (Vanhanen, 2012, pp. 31–33; cf. Vanhanen, 1999).

Ethnic Conflict is measured by the Estimated Extent of Ethnic Conflicts (EEC), an ordinal country-level index constructed from reports by international organizations and research institutes, ranging from negligible ethnic tension to large-scale ethnic violence (Vanhanen, 2012, ch. 2).

Political Terror (2017; 1 = low, 5 = high): Political Terror Scale, 1 (secure rule of law) – 5 (unlimited terror); 2017 country scores from the Political Terror Scale project (Gibney et al., 2024).

Level of Violent Crime (2017; 1 = low, 5 = high), Global Peace Index qualitative indicator “level of violent crime”, scored from 1 (very low) to 5

(very high) by Economist Intelligence Unit country analysts (Institute for Economics & Peace, 2017).

Homicide Rate (2017; per 100,000), intentional homicides per 100,000 population in 2017, from the UNODC/World Bank World Development Indicators series (World Bank, 2024c; UNODC, 2019).

Fragile State Index Rank 2023 (Fund for Peace, 2023). Higher values indicate less fragility (more stable states).

Traffic Deaths (2017; per 100,000), age-standardized mortality rate from road traffic injuries per 100,000 population in 2017 (World Bank, 2024d; WHO, 2018).

Corruption Perception Index 2023 from Transparency International's Corruption Perceptions Index (2023.). Corruption (lower = more corruption).

2.4 Photoperiod Derivation (Winter Length / Photoperiodic Hardship)

Photoperiodic hardship can be operationalized as winter-daylight deficit or winter length derived from latitude. Our reproducible approach uses the solar declination approximation and computes day length (hours) for each day of year, then summarizes the annual photoperiod deficit relative to a reference (e.g., 12 h) or counts days below a threshold (e.g., < 10 h).

- Inputs: latitude φ (radians), day-of-year d (1–365).
- Solar declination $\delta(d) \approx 0.409 * \sin(2\pi/365 * d - 1.39)$.
- Sunset hour angle $\omega s = \arccos(-\tan(\varphi) * \tan(\delta))$.

- Day length $L(d) = 24/\pi * \omega s$ (hours).
- Define deficit $D(d) = \max(0, L\_ref - L(d))$ where $L\_ref = 12$ h (or another chosen reference).
- Photoperiodic hardship = $\Sigma D(d)$ over the year (or winter months), or number of days with $L(d)$ below threshold.

Report the chosen reference/threshold and the aggregation window (annual vs winter-only). The resulting measure is then oriented so higher values indicate greater hardship and standardized with other EHI components.

2.5 Statistical handling

Analyses use Spearman rank correlations for continuous associations, Kruskal–Wallis tests for ecozone differences, and Kendall's τ for monotonic trends. Effect sizes (ε^2) are reported for group differences. All tests are two-tailed.

Part III – Model

The following model formalizes the mechanisms outlined in Part I and tested in Part II. A complete inventory of variables and equations is provided in Appendix E.

3. Variance Dynamics and Institutional Stability

3.1 Definitions

Let:

V = variance in coordination-relevant traits (x), which maps onto outcome variance Var(Y).

I = institutional stability

Empirically:

$$I \propto \frac{1}{V}$$

Variance compression under strong ecological filtering historically contributed to stable institutional environments. Under technological buffering and demographic mobility, variance may expand, potentially increasing coordination costs until new equilibria emerge.

3.2 Selection gradient

Let:

EHI = ecological harshness (Environmental Harshness Index)

T = technological buffering

S = selection gradient

Then:

$$S \propto (EHI - T)$$

As technological buffering increases, energetic filtering weakens and variance in behaviorally relevant traits may expand (Pontzer, 2017). This transformation reflects a shift in selection structure rather than a reversal of Darwinian processes.

3.3 Variance Dynamics under Energetic Constraint

Rapid demographic change may generate transitional challenges driven by variance and coordination dynamics.

$$\frac{dV}{dt} = -\alpha(EHI - T)\,V + \beta T\left(1 - \frac{V}{K}\right)$$

$$I \propto \frac{1}{V}$$

where:

V: variance in coordination-relevant traits

EHI: thermodynamic constraint

T: technological buffering

t: generational time

α, β: sensitivity parameters

K: upper bound

The first term captures selection-driven variance compression under constraint, while the second term captures variance expansion under technological buffering.

3.4 Founder effects.

Let V_0be ancestral variance and f_i the fraction of variance lost at migration step i. After k steps:

$$V_k = V_0 \prod_{i=1}^{k} (1 - f_i)$$

Founder effects reduce standing V prior to selection and interact multiplicatively with EHI-driven truncation.

3.5 Truncation Selection

Let $\boldsymbol{x}$ denote a coordination-relevant trait (e.g., cognitive efficiency, planning capacity, or metabolic regulation) with population distribution $\boldsymbol{x} \sim f(x)$ and variance $V = \mathrm{Var}(x)$.

Selection under energetic constraint operates as truncation selection, such that individuals below a viability threshold $\boldsymbol{x_c}$ are selectively removed:

$$W(x) = \begin{cases} 1 & \text{if } x \geq x_c \\ 0 & \text{if } x < x_c \end{cases}$$

where $W(x)$ is fitness.

The threshold $\boldsymbol{x_c}$ is an increasing function of thermodynamic constraint:

$$x_c = x_c(EHI)$$

with:

$$\frac{\partial x_c}{\partial EHI} > 0$$

$$x_c \propto (EHI - T)$$

Variance effect:

Repeated truncation removes the lower tail of the distribution:

$$V_{(t+1)} = \mathrm{Var}(x \mid x \geq x_c)$$

which implies:

$$V_{(t+1)} < V_{(t)}$$

even when the mean shift is modest.

Link to variance dynamics model:

This mechanism corresponds directly to the compression term as defined above, where truncation selection provides the micro-foundation for the negative term:

$$-\alpha(EHI - T)\,V$$

Under sustained constraint:

- lower-tail variants are systematically removed
- V declines across generations
- coordination-relevant traits become more homogeneous.

This produces V compression without requiring large mean shifts, consistent with the empirical decoupling of mean and V effects observed across ecozones.

3.6 Model Predictions

3.6.1 Mean constraint.

The expected value of Y varies monotonically with long-term EHI exposure:

$$E[Y] = f(EHI), f'(EHI) \neq 0,$$

where $f(')$ need not be linear and may exhibit threshold effects at ecozone boundaries.

3.6.2 Variance amplification.

Within-ecozone variance of EHI increases with absolute latitude:

$$\frac{\partial \mathrm{Var}(EHI)}{\partial \mid \mathrm{Latitude} \mid} > 0,$$

due to nonlinear photoperiodic effects, seasonal temperature volatility, and covariance among EHI components.

3.6.3 Variance inversion.

Holding mean EHI constant, outcome variance declines as environmental variance increases:

$$\frac{\partial \mathrm{Var}(Y)}{\partial \mathrm{Var}(EHI)} < 0.$$

Greater heterogeneity in ecological constraint induces truncation and coordination selection, compressing admissible outcome variance.

3.6.4 Joint variance

Outcome variance follows:

$$\mathrm{Var}(Y) = \alpha - \beta_1 EHI - \beta_2 \mathrm{Var}(EHI), \beta_1, \beta_2 > 0,$$

where α denotes baseline variance in energy-rich, low-constraint environments.

The framework predicts (i) monotonic mean shifts in Y with EHI, (ii) increasing Var(EHI) with latitude, and (iii) declining Var(Y) with both EHI

and Var(EHI). Strong variance compression may occur even when mean differences are modest, implying decoupling of mean and variance responses.

3.6.5 Falsification Conditions

The framework is challenged if:

(a) Var(Y) does not decline with Var(EHI)

(b) outcome variance increases in high-EHI, high-Var(EHI) ecozones; or

(c) Var(EHI) does not increase with latitude.

Together, these components define a thermodynamically constrained variance system governing coordination and institutional stability.

Box 1. Core Variables and Equations (MESTR Model)

Key variables

V: variance in coordination-relevant traits

EHI: environmental harshness (constraint)

T: technological buffering

S: selection gradient

I: institutional stability

α, β: sensitivity parameters

K: upper bound on variance

Core relationships

$S \propto (EHI - T)$

$dV/dt = -\alpha(EHI - T)V + \beta T(1 - V/K)$

$I \propto 1/V$

Micro-mechanism (truncation)

$W(x) = 1$ if $x \geq x_c$; 0 if $x < x_c$

$x_c \propto (EHI - T)$

$V_{(t+1)} < V_{(t)}$

Energy constraint (foundation)

$E_{total} = E_{maint} + E_{growth} + E_{repro} + E_{neural} + E_{buffer}$

$E_{surplus} = E_{in} - E_{maint}$

System logic

$EHI \uparrow \Rightarrow S \uparrow \Rightarrow V \downarrow \Rightarrow I \uparrow$

$T \uparrow \Rightarrow S \downarrow \Rightarrow V \uparrow$

Interpretation

Variance is governed by a zero-sum energetic constraint: ecological harshness compresses variance, while technological buffering expands it.

3.7. Energetic flow and allocation in the human body

3.7.1 The body as an energy allocation system

The human body is conceptualized in MESTR as an energy allocation system under constraint, where:

- Selection operates on efficiency of allocation
- Trade-offs emerge from finite metabolic capacity
- Functional systems (brain, reproduction, maintenance) compete for energy
- Long-run ecological conditions shape stable allocation patterns.

The following figure provides a biophysical representation at the organism-level foundation of the MESTR framework, linking thermodynamic constraints to life-history strategy, cognition, and ultimately societal organization.

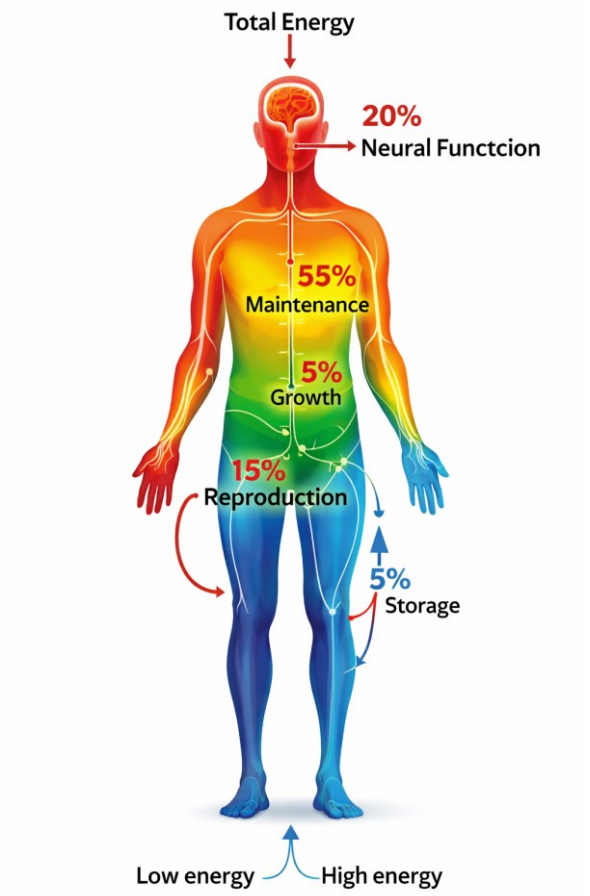

Figure 2. Energetic Flow and Allocation in the Human Body within the MESTR Framework (Author-generated schematics).

The color scale encodes relative energy density and flux:

- Red / orange → high energy demand and rapid turnover
- Yellow / green → intermediate allocation
- Blue → low immediate expenditure but potential storage or structural function.

The schematic represents the partitioning and flow of total metabolic energy (E_{total}) across major functional domains in the human organism, expressed as approximate proportions of total energy expenditure.

Energy enters the system as metabolically usable input (E_{in}) and is conserved through allocation across competing demands:

Maintenance (~55%)

- The largest share of energy is devoted to basal metabolic processes, including cellular repair, thermoregulation, immune function, and homeostasis. This domain is concentrated in the thoracic and abdominal core, reflected by warm colors (yellow–orange), indicating continuous and high energetic throughput.

Neural function (~20%)

- The brain is a disproportionately energy-intensive organ, consuming a large fraction of total energy relative to its mass. The red coloration in the cranial region indicates high metabolic density and priority allocation, consistent with the role of cognition as an energetically costly coordination system.

Reproduction (~15%)

- Energetic investment in reproductive systems and behaviors is shown in the pelvic region. This allocation varies across life-history stages and ecological conditions but represents a major competing sink within the energy budget.

Growth (~5%)

- Growth-related energy expenditure is relatively small in adults but significant during development. It is depicted centrally, reflecting its integration with systemic metabolic processes.

Storage and buffering (~5%)

- Energy reserves (e.g., adipose tissue, glycogen) function as buffers against environmental variability. Cooler colors (green–blue) in peripheral regions reflect lower immediate metabolic activity but strategic importance for stability under fluctuating conditions.

3.7.2 Allocation as micro-foundation

Figure 2 represents the organism-level energy budget underlying the MESTR framework. Total metabolically usable energy is conserved:

$$E_{total} = E_{maint} + E_{growth} + E_{repro} + E_{neural} + E_{buffer}$$

with approximate proportional allocations shown for an adult organism under moderate conditions. Color gradients encode relative metabolic flux density

(red = high, blue = low), emphasizing the concentration of energetic throughput in neural and core maintenance systems.

This allocation structure provides the micro-foundation for the variance dynamics formalized previously. Environmental harshness (EHI) acts as a constraint on net surplus:

$$E_{surplus} = E_{in} - E_{maint}$$

such that increasing EHI raises maintenance costs and reduces surplus energy available for growth, neural investment, and reproduction. This induces systematic trade-offs and contributes to the selection gradient:

$$S \propto (EHI - T)$$

where T denotes technological buffering.

At the population level, these constraints propagate into variance dynamics:

$$\frac{dV}{dt} = -\alpha(EHI - T)V + \beta T\left(1 - \frac{V}{K}\right)$$

where the compression term reflects truncation selection under energetic constraint.

The organismal allocation system depicted here constitutes the physiological basis through which ecological conditions translate into population-level variation, coordination capacity, and institutional stability. Thus, organism-level energy allocation provides the micro-mechanism through which EHI translates into population-level variance dynamics.

PART IV – Results

4. Continuous Gradients

In the following, we test our hypothesis by illustrating prehistoric adaptation to the long northernmost haul within our geographically defined masks.

4.1 EHI and Morphology

Table 3. Spearman Correlations Between the EHI and Genetic and Morphological Variables and Longitude

Variable	N	ρ	t	p
Absolute latitude (°)	78	.99	65.48	<.001
Genetic distance logit(gene probability)	43	.90	13.05	< .001
Skin color (lower = lighter)	78	.84	13.64	< .001
Genetic distance (F_{ST} or co-ancestor coefficient)	61	.84	11.67	< .001
Paleo-cranial capacity (cm^3)	78	.83	13.05	< .001
Median age (years)	78	.81	11.98	< .001
Body height (means) 1896–1996 (cm)	78	.78	10.78	< .001
Mean BMI in adults 1975–2016	78	.78	11.02	< .001
Body weight[1] (kg)	78	.65	7.47	< .001
CAG repeats (number)	42	.61	4.91	< .001
Absolute longitude (°)	78	−.18	−1.57	.12

Notes. ρ = Spearman rank correlation coefficient. t statistics correspond to tests of the correlation coefficient (df = N − 2). All correlations are computed with the EHI. [1] Calculated from body height (means) 1896-1996 and mean BMI in adults 1975-2016).

EHI shows strong monotonic associations with genetic distance, pigmentation, cranial capacity, stature, BMI, and demographic indicators (Table 3). Absolute longitude is not associated, supporting a primarily meridional signal.

These patterns indicate that EHI captures a structured gradient linking ecological constraint to biological, cognitive, and societal outcomes.

4.2 EHI and Cognition

Table 4
Spearman Correlations Between the Environmental Harshness Index (EHI) and National Cognitive Measures

Measure	N	ρ	t	p
IQ[1]	78	.82	12.57	< .001
SASIQ	37	.77	7.12	< .001
TIMSSIQ	36	.72	6.13	< .001
PIRLSIQ	32	.69	5.17	< .001
PISAIQ	32	.64	4.61	< .001

Notes. [1] Jensen and Kirkegaard (2024) used multiple sources of measured IQ and achievement tests to compute the intelligence of nations, weighted for quality but excluding dataset with geographic imputations. ρ = Spearman rank correlation coefficient. t tests correspond to df = N − 2.

SASIQ, TIMSSIQ, PIRLSIQ, and PISAIQ (Becker, 2019) is the equal-weighted average of IQ-scaled assessment means available per country; it is conceptually similar to Rindermann's (2007) 'student assessment IQ' but based on the updated country means used in the present study.

EHI shows large, positive rank associations with national measures of IQ across the full sample as with school assessments re-expressed on an IQ metric. These effect sizes indicate a robust relation between the latitudinal harshness gradient captured by EHI and cross-national cognitive performance.

4.3 EHI and societal variables

Table 5
Spearman Correlations Between the Environmental Harshness Index (EHI) and Societal Variables

Variable (societal outcome)	N	ρ	t	p
Institutional Altruism	62	.86	13.11	< .001
Scientific & Technical Journal Articles per 1,000 people	53	.85	11.34	< .001
Income Index (2023)	74	.83	12.75	< .001
Education Index (2023)	74	.83	12.66	< .001
HDI (2023)	77	.82	12.32	< .001
Achievement (2015)	69	.81	11.12	< .001
GNI per capita, 2017 PPP (2023)	77	.79	11.31	< .001
Life Expectancy Index (2023)	74	.78	10.62	< .001
Expected Years of Schooling (2023)	78	.78	10.82	< .001
Life Expectancy at Birth (2023)	78	.76	10.31	< .001
Democracy Rank Index (2023)[1]	77	.76	10.01	< .001
Gini (World Bank)	71	.60	6.20	< .001
Global Happiness	73	.48	4.62	< .001
Ethnic Heterogeneity (Vanhanen, 2012)	78	−.52	−5.35	< .001
Ethnic Conflict (Vanhanen, 2012)	78	−.62	−6.90	< .001
Political Terror (1 low – 5 high)	63	−.74	−8.63	< .001
Level of Violent Crime (1 low – 5 high)	63	−.74	−8.66	< .001
Homicide Rate (per 100,000)	63	−.75	−8.98	< .001
Traffic Deaths (per 100,000)	63	−.78	−9.69	< .001
Fragile State Index Rank (2023)	78	−.81	−12.23	< .001
Corruption Perception Index[2]	53	−.83	−10.59	< .001

Notes. ρ = Spearman rank correlation coefficient. t tests correspond to df = N − 2. [1] Lower values indicate higher democratic quality. [2] Corruption (lower = more corruption).

EHI shows strong associations with key development indicators: Positive correlations with institutional/scientific capacity and human development (e.g, Institutional Altruism, Scientific & Technical Journal Articles per 1,000 people, HDI, Education/Income indices) and negative correlations for fragility, crime, mortality, corruption and related risk metrics. These patterns mirror the latitudinal harshness gradient captured by EHI.

In summary, all main indicators in the first part of our study support the hypothesis that migrants who finally settled in the northern European ecozone after ≈ 275,000 years latitudinal migration gradually adapted to the highest levels of EHI.

4.4 Conclusion

The findings support a unified interpretation in which thermodynamic constraint structures variation across genetic, morphological, cognitive, and societal domains. Migration along energy gradients produces ordered differences in trait distributions, while technological buffering modifies variance dynamics in modern contexts.

Intelligence and civilization can thus be interpreted as thermodynamic solutions to the problem of coordinating energy under constraint. The MESTR framework provides a parsimonious bridge between evolutionary biology, human capital formation, and long-run development.

4.2 Discretized Ecozones

The second part of our hypothesis to be tested here is that migrants establishing permanent residency within one of the remaining four ecozones short of the northernmost, develop genetic adaptations over multiple

generations to the local average EHI, and slowly approach local equilibrium under sustained selection.

4.2.1 Morphology by ecozone

Table 6
EHI, Genetic Distance, and Skin Color Adaptation by Ecozone

Measure	Europe		Africa		
	N. Europe	S. Europe	Maghreb	Sahel	Equatorial
Environmental Harshness (EHI)					
Mean	85.11	65.10	38.13	17.22	7.80
SD	7.36	7.69	4.40	4.86	3.37
Genetic Distance					
F_{ST} – N	13	12	7	13	16
F_{ST} – Mean	.05	.04	.03	.02	.02
F_{ST} – SD	.00	.00	.01	.01	.01
logit(gene probability) – N	14	11	3	5	10
logit(gene probability) – Mean	1.71	1.12	-.80	-1.32	-1.44
logit(gene probability) – SD	.39	.40	.62	.65	.60
Skin Pigmentation					
N	17	15	7	17	22
Mean	1.00	1.66	5.33	6.68	6.97
SD	.000	.49	1.47	.84	.27

Notes. Ecozones ordered from high-EHI northern environments to low-EHI equatorial environments. Skin color scale coded from lighter (low values) to darker (high values).

Table 6 reports ecozone means for the PCA-weighted Environmental Harshness Index (EHI; 0–100) together with two complementary indicators

of population differentiation: genetic distance (F_{ST}) and genetic distance (logit-transformed gene probability).

Mean EHI increases monotonically from the mildest to the harshest ecozone, confirming the intended ordering of the geographically defined ecozones while also revealing non-uniform spacing that reflects empirical variation in seasonal constraint and energy limitation.

Both genetic-distance measures exhibit a systematic gradient across ecozones, with greater differentiation in harsher environments. This pattern is consistent with the MESTR interpretation that long-term ecological constraint structures the energetic and demographic context within which migration, drift, and selection jointly contribute to population-level genetic divergence. Because ecozones are defined independently of genetic outcomes and inference relies on rank-based, nonparametric tests, the observed trends cannot be attributed to linear rescaling of EHI or to latitude alone. Average skin pigmentation becomes monotonically lighter.

Group differences were evaluated with Kruskal–Wallis H-test and trends with Kendall's τ; higher values indicate greater differentiation/adaptation along the harshness gradient.

Table 7
Differences in EHI, Genetic Distance, and Skin Color Across Five Ecozones (Kruskal–Wallis Tests)

	Kruskal–Wallis Test			Trend Test		
Variable	**H (df = 4)**	**p**	**ε²**	**Kendall τb**	**Z**	**p**
EHI PCA (0–100)	72.83	< .001	.92	.89	11.49	< .001
Genetic distance from equator (F_{ST})	45.00	< .001	.70	.68	7.77	< .001
Genetic distance [logit(gene probability)]	34.69	< .001	.73	.75	7.12	< .001
Skin color	62.36	< .001	.79	.76	9.79	< .001

Note. Kruskal–Wallis tests evaluate differences among five ecozones. ε^2 denotes the nonparametric effect size. Kendall τb indicates the trend across ecozones ordered by environmental harshness (EHI).

The nonparametric omnibus group difference tests (Kruskal–Wallis, tie-corrected) demonstrate statistically significant average differences across the five ecozones. Effect sizes (ε^2) are large (with thresholds of .01 for small, .08 for medium, and .26 for large effects). Additionally, Kendall's τ_b tests confirm a positive trend, indicating increasing environmental harshness across ecozones.

4.2.2 Morphology and cognition by ecozone

Table 8
Morphology, Cognition, and Y-Haplotype Indicators by Ecozone

	Europe			Africa	
Measure	**N. Europe**	**S. Europe**	**Maghreb**	**Sahel**	**Equatorial**
Paleo-cranial capacity (cm³)					
N	17	15	7	17	22
Mean	1361	1331	1316	1303	1284
SD	21.43	11.13	21.80	23.46	20.19
IQ					
N	17	15	7	17	22
Mean	97.95	93.57	76.51	70.02	70.03
SD	1.64	4.63	4.59	4.31	4.36
Y-haplotype logit (HGSP)					
N	17	15	6	17	20
Mean	2.31	.70	-2.90	-4.26	-4.30
SD	.94	1.15	.96	1.80	1.95
Y-haplotype logit (HGSN)					
N	17	15	7	17	22
Mean	-2.72	-.95	1.36	2.01	2.31
SD	1.29	1.06	.59	1.36	1.10

Note. Ecozones ordered along the EHI gradient from northern Europe (high EHI) to equatorial Africa (low EHI). Values show means and standard deviations within ecozones.

Paleo-cranial capacity increases as the average EHI shifts from milder to harsher ecozones, and IQ means decline from European to African ecozones (approximately 98 to 70).

The average logit frequency of HGSP is markedly higher in European ecozones (approximately 2.3 in Northern Europe and 0.7 in Southern Europe)

and strongly negative in African ecozones (approximately −2.9 to −4.3). Conversely, average HGSN frequencies are strongly negative in European ecozones (approximately −2.3 and −1.0) and strongly positive in African ecozones (approximately 1.4 to 2.3).

HGSP is positively associated with higher IQ in this material N = 75, Spearman's ρ = .739, t(N-2) = 9.362, p < .001, while HGSN is negatively associated with IQ: N = 78, Spearman's ρ = -.785, t(N-2) = -11.058, p < .001.

Figure 3. Relations among EHI, Paleo-cranial capacity, IQ & Achievement by ecozone

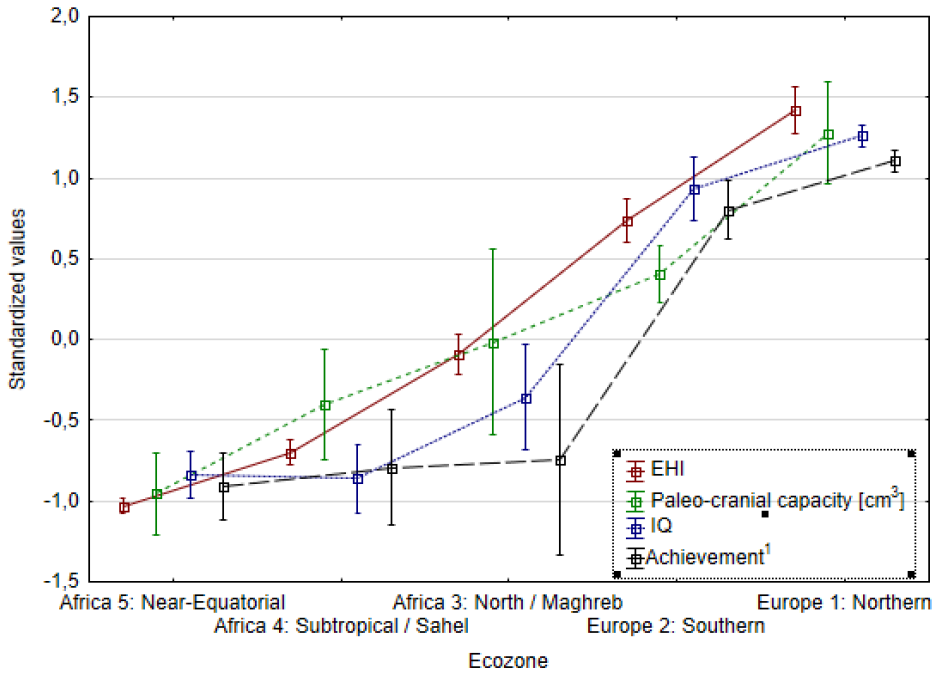

Note: [1]Meisenberg, 2015. (Author-generated schematics).

EHI increases monotonically across ecozones. This serves as a construct-validation check rather than a substantive test. Notably, the ecozone ordering was defined independently of outcome variables, reducing concerns of circularity.

Paleo-cranial capacity shows a smooth, gradual increase across ecozones, consistent with deep-time morphological differentiation along long-term thermodynamic gradients. The absence of abrupt jumps suggests cumulative adaptation rather than punctuated change.

Cognitive measures exhibit a more stepwise pattern, particularly across the North Africa–Europe transition. This divergence from the cranial-capacity curve is informative and indicates that contemporary cognitive outcomes are not simple linear reflections of morphology, but may reflect later historical, cultural, or institutional amplification layered onto earlier biological differences.

Achievement outcomes broadly track IQ but with greater dispersion, as expected. Their alignment with the ecozone ordering nonetheless strengthens external validity by showing that the cognitive gradient has downstream correlates in real-world performance indicators.

Table 9
Differences in Morphological, Cognitive, and Genetic Indicators Across Five Ecozones

	Kruskal–Wallis Test			Ordered Ecozone Trend		
Variable	H (df = 4)	p	ε^2	Kendall τb	Z	p
Paleo-cranial capacity (cm^3)	51.20	< .001	.63	.71	9.21	< .001
IQ	60.51	< .001	.76	.69	8.92	< .001
Logit (Y-haplotype HGSP)	57.17	< .001	.73	.67	8.50	< .001
Logit (Y-haplotype HGSN)	57.53	< .001	.72	-.68	-8.84	< .001

Table 9 shows that the ecozone grouping captures substantial and highly ordered average differences in both morphology, cognition, and haplotypes. Thus Kruskal–Wallis tests are all highly significant. The ε^2 values (≈0.63–0.76) indicate that around two-thirds to four-fifths of the variance in these variables is attributable to ecozone membership—far beyond small or moderate effects. Trend tests (Kendall's τ_b ≈ .67–.71, all p < .001) show strong ordering between the five ecozones, as expected under the model, with the hypothesized gradient from near-equatorial Africa to northern Europe, with HGSN declining and HGSP increasing. In other words, average paleo-cranial capacity, IQ, and IQ-related gene frequencies do not just differ between zones; they change systematically across the ecozone harshness sequence.

4.2.3 Fertility by ecozone

Table 10
Testosterone Sensitivity, Fertility, and Morphological Indicators by Ecozone

Measure	N. Europe	S. Europe	Maghreb	Sahel	Equatorial
CAG repeats (androgen receptor sensitivity)					
N	14	13	5	3	7
Mean	22.02	21.60	19.52	18.85	19.61
SD	.54	.78	1.73	2.03	1.98
Birth rate (per 1,000)					
N	17	15	7	17	22
Mean	10.74	10.23	22.26	35.09	34.14
SD	1.36	2.53	4.28	6.81	4.83
Mother age at first birth					
N	17	15	7	17	22
Mean	28.38	28.26	22.11	19.99	21.09
SD	1.32	2.09	2.59	1.80	2.66
Body height (cm, 1896–1996 means)					
N	17	15	7	17	22
Mean	168.75	165.55	162.18	163.05	161.73
SD	1.51	2.22	.90	2.09	1.20

Table 10 shows that average CAG-repeat number, fertility, maternal age at first birth, and adult height all differ systematically across ecozones. CAG repeats in the androgen receptor gene (a rough proxy for androgen sensitivity; the more, the lower) are highest in the northern and southern European ecozones and lower in the African ecozones. Average birth rates display the opposite pattern: low in Europe and substantially higher in the Maghreb, Sahel, and near-equatorial Africa. Average maternal age at first birth is about 28 years in Europe but roughly 20–22 years in the African ecozones. Average

adult height is greatest in northern Europe, somewhat lower in southern Europe, and lowest on average in the African ecozones.

Table 11
Differences in Testosterone Sensitivity, Fertility, and Morphology Across Five Ecozones

Variable	Kruskal–Wallis Test			Ordered Ecozone Trend		
	H (df = 4)	p	ε^2	Kendall τb	Z	p
CAG repeats (androgen receptor sensitivity)	20.21	< .001	.40	.51	4.73	< .001
Birth rate (per 1,000 population)	61.16	< .001	.77	-.60	-7.79	< .001
Mother age at first birth (2006–2015)	52.51	< .001	.65	-.52	-6.75	< .001
Body height (cm; 1896–1996 means)	51.22	< .001	.63	.62	8.06	< .001

Table 11 confirms that these average differences are statistically strong and ordered. Kruskal–Wallis tests are all significant at $p < .001$, with medium to large effect sizes. Kendall's τ_b indicates a across-ecozone average trend: CAG repeats and height increase from near-equatorial Africa toward northern Europe, whereas birth rates and maternal age at first birth decrease along the same sequence.

These patterns fit well with a life-history interpretation within MESTR: the on-average harsher ecozones (shorter growing seasons, greater thermal

seasonality, higher energetic constraints) are associated with later reproduction, lower fertility, greater stature, and reduced androgen sensitivity, as predicted, with a slower, more investment-intensive reproductive strategy across generations.

4.2.4 Longevity, Education, and Happiness by ecozone

Table 12: Longevity, Education, Achievement, and Happiness by Ecozone

Measure	N. Europe	S. Europe	Maghreb	Sahel	Equatorial
Life expectancy at birth (2023)					
N	17	15	7	17	22
Mean	80.27	80.10	67.82	64.77	63.26
SD	2.71	3.94	7.52	3.77	3.55
Expected years of schooling					
N	17	15	7	17	22
Mean	17.25	16.30	13.44	9.60	10.47
SD	1.79	1.82	1.52	1.61	1.87
Education index					
N	17	14	6	17	20
Mean	.90	.84	.66	.43	.47
SD	.04	.07	.07	.12	.11
Achievement (2015)					
N	17	15	7	14	16
Mean	98.33	94.03	72.00	71.31	69.67
SD	1.98	4.69	9.07	8.83	5.64
Global happiness					
N	17	15	7	16	18
Mean	218.65	208.13	169.00	164.69	170.22
SD	43.82	42.36	21.68	26.87	24.07

Table 12 presents ecozone means for longevity, educational attainment, cognitive/educational achievement, and subjective well-being across geographically defined ecozones.

Across indicators, outcomes exhibit systematic gradients by ecozone, with populations in harsher ecozones showing, on average, higher longevity, educational investment, achievement, and self-reported well-being. Importantly, the spacing between ecozones is not uniform, reflecting the empirically derived nature of EHI and variation in seasonal constraint and energy limitation within latitude bands. These patterns are consistent with the MESTR framework, which interprets long-term ecological harshness as a distal constraint shaping the energetic, demographic, and institutional environments within which human capital accumulation and societal outcomes emerge. Again, because ecozones are defined independently of the outcome variables and inference relies on rank-based, nonparametric tests, the observed gradients cannot be reduced to linear rescaling of EHI or to latitude alone.

Table 13
Differences in Sociological Indicators Across Five Ecozones

	Kruskal–Wallis Test			Ordered Ecozone Trend		
Variable	H (df = 4)	p	ε^2	Kendall τ_b	Z	p
Life expectancy at birth (2023)	56.41	< .001	.70	.61	7.93	< .001
Expected years of schooling (2023)	60.00	< .001	.75	.62	8.03	< .001
Education index (2023)	58.77	< .001	.78	.67	8.45	< .001
Achievement (2015)	51.53	< .001	.72	.65	7.94	< .001
Global happiness (2015)	20.95	< .001	.23	.36	4.46	< .001

Table 13 confirms that these average differences are large and statistically robust. Kruskal–Wallis tests yield H values between ≈52 and 60 for life expectancy, schooling, education index, and achievement, all $p < .001$, with substantial effect sizes ($\varepsilon^2 \approx .7–.8$). Ecozone membership thus explains around three quarters of the variance in these outcomes. Kendall's τ_b values ($\approx|.61–.67|$, all $p < .001$) indicate strong trends across the five ecozones, as expected under the model, with the hypothesized ecozone ordering from near-equatorial Africa to northern Europe. Average global happiness also differs by ecozone, but with a more modest effect ($\varepsilon^2 \approx .25$), suggesting that subjective happiness is less tightly constrained across the ecozone gradient than longevity, education, and cognitive achievement. In MESTR terms, these results indicate that ecozones capturing long-term average environmental harshness also sort populations by mean life expectancy, educational investment, and cognitive performance, extending the energetic gradient from biology into key components of human capital.

4.2.5 Societal and Institutional Outcomes by ecozone

Table 14
Societal Outcomes by Ecozone

Measure	N. Europe	S. Europe	Maghreb	Sahel	Equatorial
Income index (2023)					
N	17	14	6	17	20
Mean	.95	.91	.71	.53	.53
SD	.05	.07	.10	.11	.12
Human Development Index (2023)					
N	17	14	6	17	20
Mean	.93	.89	.70	.53	.55
SD	.04	.06	.07	.09	.08
Democracy rank index (2023) [1]					
N	17	15	7	17	21
Mean[1]	27.88	40.53	105.29	111.71	119.52
SD	34.99	22.84	37.87	36.79	28.24
Scientific & technical journal articles					
N	15	14	5	7	12
Mean	47.62	32.11	2.74	1.51	1.20
SD	27.12	25.34	1.87	.63	.20
Fragile State Index rank (2023) [2]					
N	17	15	7	17	22
Mean[2]	157.35	140.67	63.14	41.76	37.64
SD	22.50	25.36	24.74	34.54	28.42

Note. [1] Lower values indicate higher democratic quality. [2] Higher values mean more stable.

Table 14 extends the ecozone analysis to societal and institutional indicators. Average income index and HDI are highest in the European ecozones, lower in the Maghreb, and lowest in the Sahel and near-equatorial Africa. The

democracy rank index (lower values = more democracy) shows the same ordering: more democratic systems in Europe, less democratic systems in the African ecozones. Scientific and technical journal articles per 1,000 people are dramatically more frequent in Europe than in Africa. The Fragile State Index rank, where higher rank denotes greater stability, likewise favors the European ecozones and declines toward the Sahel and near-equatorial ecozones.

Table 15
Differences in Societal Outcomes Across Five Ecozones

	Kruskal–Wallis Test			Ordered Ecozone Trend		
Variable	**H (df = 4)**	**p**	**ε²**	**Kendall τb**	**Z**	**P**
Income index (2023)	56.16	< .001	.74	.65	8.20	< .001
Human Development Index (2023)	60.69	< .001	.76	.66	8.22	< .001
Democracy rank index (2023)	46.23	< .001	.57	.57	7.36	< .001
Scientific & technical journal articles per 1,000 people	40.10	< .001	.73	.71	7.45	< .001
Fragile State Index rank (2023)	56.24	< .001	.70	.64	8.30	< .001

Table 15 shows that these average ecozone effects are large and highly significant. Kruskal–Wallis H values for income index, HDI, democracy rank, scientific output, and fragile state are all substantial ($H \approx 40–61$, $p < .001$), with ε^2 in the .57–0.76 range, again indicating that ecozone membership accounts for well over half the variance in these outcomes. Kendall's τ_b values ($\approx|.57–.71|$, all $p < .001$) confirm strong trends across ecozones from near-equatorial Africa through the Sahel and Maghreb to southern and northern Europe.

Ecozone analyses confirm ordered differences across five bands from near-equatorial Africa to northern Europe. EHI, genetic distance, pigmentation, cranial capacity, IQ, and societal indicators increase monotonically across ecozones (Tables 6–15), with considerable effect sizes and strong trend statistics.

Ecozones are defined independently of outcomes; inference relies on nonparametric tests, reducing sensitivity to scaling and distributional assumptions. The results indicate cumulative differentiation consistent with long-run adaptation to local constraint.

.

PART V – Discussion

5.1 Environmental harshness and genetic differentiation

The present framework differs from earlier single-variable climate or "cold-winter" models by treating environmental harshness as a composite energetic constraint rather than a single climatic driver. Ecozones are defined independently of outcome variables, and analyses rely primarily on rank-based statistics robust to rescaling. EHI therefore functions as a thermodynamic descriptor that contextualizes long-term population patterns within migration history, energetic allocation, and institutional development.

This study asked whether recent evolution in human intelligence and civilization can be interpreted within an explicitly energetic framework. Using the Environmental Harshness Index (EHI; higher = harsher) and a five-band ecozone scheme across the Afro–European corridor, we related environmental conditions to genetic, morphological, cognitive, life-history, and societal variables. In Part 1 results, EHI was treated as a continuous predictor; in Part 2 results, the same gradient was discretized into ecozones.

Across both approaches, a consistent pattern emerged: populations exposed to harsher environments—with longer and darker winters, stronger thermal seasonality, colder minima, and lower irradiance—tend to show greater genetic differentiation from equatorial references, systematic shifts in morphology and life-history, higher average cognitive performance, and more favorable societal indicators. With EHI discretized into ecozones (Table 2), we evaluated effects of taking permanent residency at different distances

from the Equator and the results suggested gradually approaching polygenic fixation over multiple generations to various average EHI levels.

5.2 Genetic and morphological life-history adjustments

Genetic distances from equatorial reference populations increase monotonically with EHI and across ecozones from near-equatorial Africa to northern Europe. Continuous EHI correlations are large, and ecozone Kruskal–Wallis tests with strong trend statistics show strict ordering along the harshness sequence. These findings are compatible with serial founder effects during northward migration, compounded by many generations of local selection.

Morphological traits follow the same ordered pattern. Skin pigmentation lightens with increasing EHI and ecozone harshness, consistent with UVR and photoperiod constraints on vitamin D synthesis and folate protection. Paleo-cranial capacity is larger on average in harsher ecozones, in line with ecogeographic work linking brain size to climate. Stature and body weight/BMI also tend to increase with latitude and harshness, matching thermoregulatory principles and modern nutritional gradients. Life-history markers add further structure: androgen receptor CAG-repeat length, used here as a coarse proxy for androgen sensitivity, shows higher mean values (implying lower effective testosterone sensitivity) in European ecozones than in African ecozones. Fertility is low and maternal age at first birth high in Europe, whereas the Maghreb, Sahel, and near-equatorial ecozones show higher birth rates and earlier first births. Medium-to-large ecozone effect sizes and strong trend tests suggest a shift toward a slower, more investment-intensive life-history strategy in harsher environments.

Continuous EHI correlations are large, and ecozone-based Kruskal–Wallis tests confirm strict monotonic ordering across the harshness gradient. Together, these results indicate that ecological constraint structures both central tendencies and variance distributions.

Within the MESTR framework, this pattern is taken to indicate that energy constraints and climatic demands have helped structure the genetic landscape in ways that reflect cumulative adaptation to regional energetic regimes.

5.3 Cognitive outcomes and Y-haplogroup structure

National cognitive performance—both the Jensen & Kirkegaard IQ index and student assessment scores (SASIQ, TIMSSIQ, PIRLSIQ, and PISAIQ) are positively associated with EHI (Table 4). Ecozone comparisons likewise show large between-zone-differences, with ordered increases from near-equatorial Africa through intermediate Ecozones to northern Europe (Table 8).

Within MESTR, general intelligence is interpreted as a costly adaptation for planning and coordination whose marginal value rises under energetic uncertainty and seasonal constraints. Y-haplogroup composition shows a convergent pattern: ecozone frequencies of the HGSP set are high in the northern and southern European ecozones and strongly negative in the African ecozones, whereas the HGSN set shows the mirror distribution (Table 8). Mean IQ declines from the European to the African ecozones, such that HGSP is positively aligned with IQ and HGSN negatively aligned. This reproduces, in an ecozone framework, the pattern reported by Rindermann, Woodley, and Stratford (2012). Here, HGSP and HGSN are treated as coarse markers of deep ancestry whose thermodynamic associations with IQ are

compatible with—but not definitive proof of—long-term selection on intelligence-related traits.

5.4 Societal indicators and macro-social outcomes

Societal-level variables display similar ordering. In the continuous analyses, EHI correlates positively with indices of human development and institutional capacity (HDI), income index, education index, life expectancy, scientific and technical output, and institutional altruism) and negatively with fragility, corruption, violent crime, political terror, and homicide rates. Ecozone analyses show that income, HDI, democracy, life expectancy, and scientific productivity are highest in the European ecozones, intermediate in the Maghreb, and lowest in the Sahel and near-equatorial ecozones, with large effect sizes and monotonic trends (Tables 12 and 14). These gradients suggest that the energetic and cognitive adaptations associated with harsher environments may scale up into institutional performance and macro-social functioning. At the same time, they are not interpreted as simple climatic determinism: the societal patterns are seen as downstream correlates of long-term interactions between ecological constraints, evolved trait distributions, demography, and historical contingencies.

Several limitations should be noted here, however. First, the analyses are ecological and rely on country-level aggregates, which may obscure within-population heterogeneity. Second, causal inference remains constrained by historical and institutional confounding factors not fully captured by EHI. Third, genetic and cognitive proxies are indirect and subject to measurement and interpretation uncertainty. The results should therefore be interpreted as

macro-structural patterns consistent with energetic constraints, rather than definitive causal estimates

5.5 Variance inversion under MESTR: founder effects, truncation selection, and canalization

Within the MESTR framework, the observed variance inversion arises from the interaction of serial founder effects, truncation selection, and canalization under persistent energetic constraint. Founder effects reduce standing variance during migration, truncation selection removes low-robustness variants, and canalization stabilizes viable phenotypes under volatile energetic conditions. Consequently, increasing environmental variance is associated with decreasing outcome variance, producing the mirror pattern predicted by the model. In the formal derivations, V denotes coordination-relevant variance, operationalized empirically as dispersion in behavioral, cognitive, and institutional outcome distributions.

5.6 Cold Winter theory and MESTR

Earlier cold-climate and winter-severity theories proposed that prolonged exposure to cold temperatures directly selected for higher intelligence or cognitive complexity. While winter conditions capture one important dimension of thermodynamic stress, such single-variable models do not specify how energetic costs are allocated across growth, maintenance, reproduction, and cognition under constrained metabolic budgets. In contrast, the present MESTR framework and EHI treat cold exposure as one component within a broader energetic system that also includes photoperiodic constraint, seasonal energy availability, and ecological productivity. This

integrative approach aligns with metabolic models emphasizing energetic allocation trade-offs rather than direct climatic causation and avoids attributing population-level patterns to any single environmental factor.

5.7 Demographic Transition and Technological Buffering

Industrialization and technological development altered the ecological landscape by buffering environmental constraint. Mortality risks declined, resource volatility diminished, and welfare systems reduced the survival penalties associated with ecological harshness. Selection did not cease, but its gradient weakened and changed direction (Nyborg, 2011).

Institutions function as energetic coordination regulators, buffering ecological constraint through redistribution, administrative mediation, and risk pooling.

As technological buffering approaches or exceeds ecological harshness, energetic filtering weakens, and variance in coordination-relevant traits may expand. This transition represents a transformation of selection structure under altered energetic conditions.

5.8 Transitional Challenges Under Rapid Demographic Change

Rapid demographic change can produce temporary structural challenges even in historically stable systems. These challenges arise primarily from variance and coordination dynamics.

5.9 Coordination Costs

Complex institutions require predictable behavior, stable norms, and low variance in coordination-relevant traits. If demographic transitions increase variance faster than institutional adaptation occurs, coordination costs may rise, affecting governance, labor markets, and educational systems.

5.10 Integration Lag

Assimilation typically unfolds across multiple generations. During transitional phases, incomplete cultural transmission, genetic and educational heterogeneity, and socioeconomic and demographic stratification may temporarily widen variance, increasing institutional load.

5.11 Institutional Adaptation

Institutional resilience depends on the rate of demographic change relative to the rate of adaptation. Historical evidence reflects that societies undergoing rapid demographic transformation often experience transitional instability before reaching a new equilibrium.

5.12 Implications and future directions

Viewed together, our findings form a structured energetic gradient. As populations moved away from the equator into regions with shorter growing seasons, stronger thermal seasonality, they underwent cumulative changes in genetic composition, morphology, life-history, and behavior that improved their ability to manage energy under more demanding conditions. Populations residing in high-EHI ecozones tend to show higher average scores on

measures of general intelligence and student achievement, along with more favorable life-history and societal profiles (Tables 8–11); at the societal level, it is reflected in higher average levels of human development, institutional capacity, and stability (Tables 12–15).

Within the MESTR (Migration–Energy Selection–Trait Redistribution) framework, these patterns are interpreted as the outcome of optimization under energy scarcity (captured indirectly via irradiance): traits that enhance efficient energy capture, long-term planning, coordination, and regulation are gradually favored in harsher ecozones. Our hypothesis is supported insofar as populations residing in high-EHI northern ecozones show consistent signals of cumulative differentiation in genetic, morphological, cognitive, and societal domains. It is further supported insofar as average ecozone membership explains a large share of the geographically local variances in key traits and variables, following ordered gradients across the five ecozones.

Empirically, the study highlights several directions for future work. Ancient-DNA data can be used to test whether the inferred ecozone differences in genetic structure and cranial morphology were present in ancestral populations at specific times and locations. Multi-level designs combining individual-level cognitive data, genome-wide polygenic scores, and finely resolved environmental indicators could help separate genetic, developmental, and institutional contributions to present-day differences. Improved paleoclimate reconstructions and historical datasets would allow EHI to be extended back in time, testing the stability of the energetic gradient. Formal energetic modelling could explore the conditions under which energy-related selection pressures produce gradients of the magnitude observed here.

The observed patterns arise from many interacting forces: prehistoric selection and drift, post-glacial recolonizations, steppe expansions, colonial and post-colonial history, modern education and health systems, and globalized trade and technology.

MESTR offers an energetic backbone for organizing these processes without claiming to specify every causal pathway. Conceptually, the results suggest that starting from energy flows, metabolic budgets, and thermodynamic constraints can help integrate findings from genetics, anthropology, psychology, and development economics. By emphasizing energetic allocation and thermodynamic constraint rather than proximate cultural or political explanations, the MESTR framework thus offers a parsimonious, testable backbone for integrating human biological evolution with long-term patterns of cognitive and institutional development.

MESTR is consistent with Ludwig Boltzmann's view that Darwin's theory is on a par with the mechanical theory of heat and that even the most complex biological phenomena will ultimately be captured in physical–chemical formulas (Boltzmann, 1886/1974, 1979, pp. 29, 41; Lotka, 1922; Nyborg, 1994, 1997; Odum, 1996; Schuster, 2007). The latter emphasizes that Boltzmann anticipated key elements of modern evolutionary thinking by framing biological organization as a consequence of differential persistence under energy-flow constraints, an interpretation grounded in Boltzmann's late philosophical writings.

Taken together, the results support a unified interpretation in which ecological constraint, energetic allocation, and variance dynamics jointly

shape biological evolution and institutional development. Migration along environmental gradients produce structured variation in genetic and phenotypic traits, while technological buffering modifies these dynamics in modern contexts. The MESTR framework thus provides a parsimonious bridge between evolutionary biology, human capital formation, and long-run economic development, grounded in general energetic principles.

5.13 Empirical limitations

Linking energy flows, climate, metabolism, cognition, and societal development across tens of thousands of years raises multiple conceptual, empirical, and statistical challenges. Several limitations should therefore be emphasized.

5.13.1 Geographic scope and masking

The analysis is restricted to an Afro–European mask and infers long-run processes from contemporary data. Haplogroup measures capture partial genetic structure; phenotypic indicators reflect both historical and modern influences; and country-level analyses do not imply individual-level causation.

EHI is correlated with latitude and related variables, and societal indicators are interdependent; results therefore emphasize effect sizes and monotonic trends rather than causal identification.

The framework should be understood as a high-level energetic model requiring further testing with ancient DNA, individual-level data, and refined paleoenvironmental reconstructions.

A strong EHI–IQ association observed worldwide (e.g., ρ ≈ .75 across all countries) indicates that similar patterns likely exist outside the mask, but they are not quantified here.

5.13.2 Temporal mismatch and retrospective inference

The study infers prehistoric selection from modern data. EHI is constructed from recent climatological baselines and outcome variables include contemporary IQ scores, fertility rates, institutional indices, and health indicators. While the broad spatial pattern of environmental harshness is likely to have remained relatively stable over late Quaternary timescales, demographic densities, technology, trade networks, and institutions clearly have not. The use of modern aggregates to infer long-term adaptive responses is therefore indirect. That said, several lines of evidence suggest temporal continuity at a coarse level—for example, the similarity between historical and modern IQ distributions across descendant populations and the persistence of steppe and post-glacial ancestry components—but these do not remove the need for caution.

5.13.3 Genetic data constraints

Y-chromosome haplogroups capture only paternal lineages and are, together with maternal mitochondrial haplogroups, sensitive to drift, founder effects, and sex-biased migration. They do not capture the full autosomal or mitochondrial genome or the complexity of polygenic architectures relevant for cognition, morphology, or life-history traits. Likewise, ecological summaries of androgen receptor CAG repeat distributions are based on relatively small and heterogeneous samples, often from convenience populations, and apply only to males. These constraints limit the precision

with which specific genetic mechanisms can be identified, and they make any strong claims about causal pathways premature.

5.13.4 Phenotypic and fossil data limitations

The cranial-capacity dataset combines pre-colonial samples from widely varying time periods and locations, later geo-linked to modern country borders. This introduces potential mismatch between fossil sampling frames and present-day populations. Anthropometric indicators (height, weight, BMI) are influenced by modern nutrition, urbanization, disease burden, and public health. Although ecozone and EHI gradients are evident in these data, they reflect a mixture of historical selection, recent environmental improvements, and secular trends.

5.13.5 Level of analysis

The analyses operate at the level of countries and ecozones. Correlations between national-level EHI and national-level IQ or institutional indices do not automatically translate into individual-level causal relationships. Subnational variation, urban–rural differences, and micro-level heterogeneity are not captured. In principle, multi-level designs with individual and regional data, as well as fine-grained genetic information, would be needed to test the MESTR hypotheses more directly.

5.13.6 Collinearity and statistical dependence

EHI is strongly correlated with absolute latitude, UVR, photoperiod, and temperature. Many societal indices are intercorrelated as well. This collinearity complicates attempts to assign unique explanatory weight to any single component. In addition, neighboring countries are not statistically independent units due to shared history, migration, and trade. The present

results therefore emphasize effect sizes, monotonic trends, and robustness checks rather than formal causal identification.

5.13.7 Multiple testing and model uncertainty

The study examines a large number of correlations and group comparisons. Although the observed effect sizes are typically large and consistent with priori directional expectations, the risk of chance findings remains. Adjustments for multiple testing (e.g., false discovery rate control) and pre-registration of key hypotheses would strengthen future work. Likewise, alternative model specifications—using different ecozone boundaries, weighting schemes, or environmental composites—should be explored.

5.13.8 Mechanistic incompleteness

MESTR proposes that energy constraints and climatic harshness shape polygenic trait distributions and, ultimately, civilizational outcomes. However, the detailed pathways from genotype to phenotype to institution remain only partially mapped, especially for complex traits such as general intelligence or cooperative behavior. Current genetic studies have identified many loci associated with cognitive and educational outcomes, but they explain only a fraction of the variance and are mostly derived from contemporary populations. The present framework should therefore be viewed as a high-level energetic model that awaits more precise mechanistic elaboration.

Taken together, these limitations imply that the results are best interpreted as evidence for broad, structured covariation between environmental harshness, genetic and phenotypic traits, and societal indicators, rather than as definitive proof of specific causal mechanisms. Future work combining ancient DNA,

high-resolution paleo-climate reconstructions, individual-level cognitive data, and formal energetic modelling will be required to test the MESTR framework more rigorously.

5.13.9 Scope and interpretation

The present work is explicitly population-level and retrospective. It does not address individual variation, individual causation, or policy prescriptions. All results describe long-term statistical regularities shaped by migration history, energetic constraints, and interacting biological and institutional processes.

The MESTR framework is therefore best understood as an organizing model rather than a complete causal theory. It provides a thermodynamically grounded backbone for integrating diverse findings across genetics, anthropology, psychology, and development studies, while leaving substantial room for refinement, extension, and falsification. Future work should be seen not as confirmation of fixed conclusions, but as progressive elaboration of the energetic mechanisms sketched here.

The preceding sections established how ecological constraint structures biological and societal variation across ecozones. We now extend this framework to contemporary systems, where technological buffering and demographic change alter the variance structure and impose new coordination demands on institutions.

5.14 Genetic Diversity, Assimilation, and Institutional Dynamics

5.14.1 Emergent energetic costs of diversity

A key implication of the framework is that genetic and cultural heterogeneity impose emergent energetic costs. These costs scale nonlinearly with population size and institutional complexity. Assimilating genetically and behaviorally dissimilar groups requires sustained investments in enforcement, signaling, and conflict management. In harsh environments, such investments divert energy from reproduction, innovation, and maintenance, reducing long-run adaptive capacity.

5.14.2 Assimilation, similarity, and long-run outcomes

The association between genetic similarity, assimilation, and higher cognitive and institutional outcomes reflects differences in energetic efficiency under constraint. Populations facing chronic scarcity cannot afford persistent coordination losses. Over evolutionary time, this favors trait bundles—cognitive, behavioral, and institutional—that enhance predictability, conformity, and long-term planning. Persistent energetic constraint thus selects for coordination-stabilizing traits, including planning depth, reliability, and institutional compatibility.

5.14.3 Interaction between migration, genetic distance, and assimilation

MESTR predicts a systematic pattern: Early migrants leaving equatorial Africa experience serial founder effects. These effects increase genetic distance from the source population while simultaneously reducing within-group diversity. Reduced diversity facilitates faster assimilation, because fewer incompatible behavioral and physiological variants must be

coordinated. In turn, assimilation enhances social cohesion, long-term planning, and cumulative cultural complexity.

This mechanism aligns with our empirical findings: increasing genetic distance from the equator, increasing EHI, increasing cranial capacity, increasing cognitive performance, increasing institutional achievement.

None of these steps require invoking genetic determinism at the individual level.

5.14.4 Why the effect strengthens with ecological harshness

In benign environments surplus energy can mask inefficiencies, heterogeneity is less costly, and coordination failures are survivable.

In harsh environments: margins are thin, coordination failures are lethal, inefficient group structures are selected against.

Thus, MESTR predicts that: the adaptive value of genetic similarity and assimilation increases monotonically with ecological harshness. This prediction is consistent with the EHI gradients, ecozone results, genetic distance correlations, and the divergence between Africa and Europe.

5.14.5 Consequences for intelligence and civilization

Within this framework: General intelligence is not selected in isolation, but as a central part in a nexus of a bundle of traits (Jensen, 1998) that improve: planning, abstraction, norm enforcement, and coordination under constraint.

Assimilated populations with high internal similarity can: sustain more complex institutions, transmit knowledge more faithfully, accumulate technological and administrative capital over generations.

5.15 Historical Clustering of Intellectual Achievement

5.15.1 Human Accomplishment

Earlier demographic-evolutionary work indicates that certain pre-industrial European populations may have experienced directional selection associated with socio-economic stratification, urbanization, and the diffusion of behavioral norms. Related hypotheses in economic history have proposed that differential fertility linked to literacy, numeracy, and market participation may have influenced population composition over long periods (Clark, 2007).

Charles Murray's *Human Accomplishment* (2003) identifies a marked historical clustering of eminent intellectual and creative achievements in Western Europe between roughly 1400 and 1950. Across scientific, philosophical, and artistic domains, a comparatively small geographic region generated a disproportionately large share of individuals later recognized as historically significant.

Table 16.

Forty eminent northwestern males, out of 4.000+.

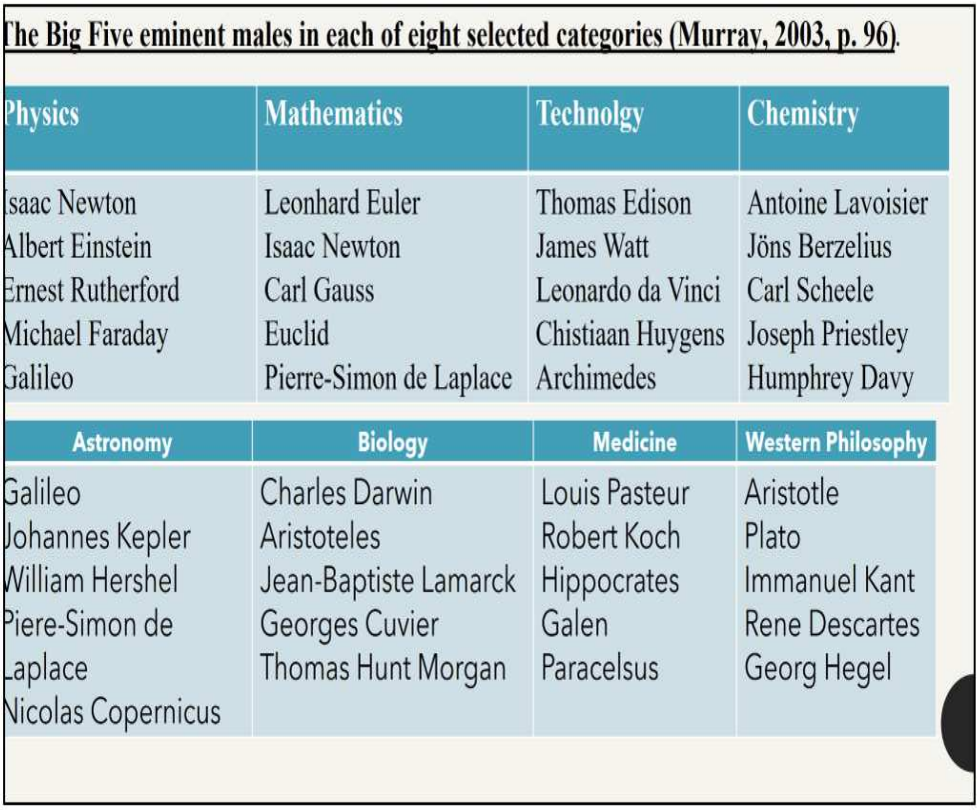

The Big Five eminent males in each of eight selected categories (Murray, 2003, p. 96).

Physics	Mathematics	Technolgy	Chemistry
Isaac Newton	Leonhard Euler	Thomas Edison	Antoine Lavoisier
Albert Einstein	Isaac Newton	James Watt	Jöns Berzelius
Ernest Rutherford	Carl Gauss	Leonardo da Vinci	Carl Scheele
Michael Faraday	Euclid	Chistiaan Huygens	Joseph Priestley
Galileo	Pierre-Simon de Laplace	Archimedes	Humphrey Davy

Astronomy	Biology	Medicine	Western Philosophy
Galileo	Charles Darwin	Louis Pasteur	Aristotle
Johannes Kepler	Aristoteles	Robert Koch	Plato
William Hershel	Jean-Baptiste Lamarck	Hippocrates	Immanuel Kant
Piere-Simon de Laplace	Georges Cuvier	Galen	Rene Descartes
Nicolas Copernicus	Thomas Hunt Morgan	Paracelsus	Georg Hegel

All these geniuses were born or worked in the globally tiny polygon of western Europe between years -800 unto 1950. Their successors eventually brought their genetic signature, culture, and civilization with them to the United States and other then developmental countries.

Within the MESTR framework, this clustering is interpreted not as evidence of immutable group hierarchy but as the outcome of long-run alignment

between ecological constraint, demographic continuity, and institutional stability. Ecological harshness can influence selection pressures, variance structure, and coordination demands, thereby shaping the conditions under which cumulative cultural and institutional development becomes possible.

Where energetic filtering compresses variance in traits relevant to coordination and long-term planning, coordination costs decline and institutional continuity becomes more stable. Under such conditions, cumulative innovation may accelerate, producing historical clustering of achievement.

The explanatory question is therefore structural: Under what ecological and demographic conditions does variance in cognitively and organizationally demanding traits become stabilized or compressed across generations?

5.16 The Danish Case

5.16.1 Institutional Systems, Energetic Constraint, and MESTR Dynamics

Denmark represents a high-coordination institutional system that historically evolved under relatively strong ecological constraint and low variance. Within the MESTR framework, such systems operate near coordination optimum, where institutional efficiency depends on maintaining low dispersion in coordination-relevant traits.

Institutional stability depends inversely on coordination-relevant variance:

$$\mathrm{C} \propto \mathrm{V}$$

where C denotes coordination cost and V variance in coordination − relevant traits.

When variance remains low, coordination costs are minimized and institutions operate near energetic efficiency.

Assimilation introduces an additional variance component that perturbs this equilibrium.

5.16.2 Variance Structure and Institutional Load

Let institutional variance be decomposed as:

$$V_{total} = V_H + V_I + V_{between}$$

Where:

V_H: host population variance

V_I: internal variance within incoming population

$V_{between}$: variance between host and incoming institutional-behavioral distributions

Coordination cost increases approximately proportionally:

$$C_{coord} = \alpha V_{between}$$

In historically low-variance systems such as Denmark, institutions operate close to coordination optimum; therefore even moderate increases in $V_{between}$ produce disproportionate administrative and institutional load.

5.16.3 Energetic Cost Function (MESTR Extension)

Assimilation cost must be modelled as a systemic energetic burden rather than purely fiscal expenditure:

$$E_{assim} = C_{coord} + C_{buffer} + C_{admin}$$

Where:

C_{coord}: enforcement, legal mediation, regulatory oversight

C_{buffer}: welfare and integration buffering

C_{admin}: institutional complexity and administrative expansion

Fiscal transfers are only observable manifestations of deeper energetic coordination load.

5.16.4 Welfare State as Buffering Mechanism

Denmark's welfare state functions as a technological buffering system that absorbs variance differential through institutional intervention. Buffering mechanisms include:

- language and education adaptation
- labor-market integration policies
- income stabilization during assimilation lag
- social redistribution and housing adjustment
- expanded administrative mediation

Buffering reallocates institutional energy within a bounded system. Total systemic energy is finite; increased buffering requires reallocation from other functions.

5.16.5 Dynamic Convergence Model

Hard environments make people similar and coordinated; easy environments allow diversity but require stronger institutions to manage it. Assimilation is a time-dependent convergence process:

$$\frac{dV_{between}}{dt} = -\lambda V_{between} + \delta$$

Where:

λ: convergence (integration) rate

δ: structural variance inflow

Equilibrium variance:

$$V^*_{between} = \frac{\delta}{\lambda}$$

If convergence dominates inflow, institutional load declines over time; if not, elevated coordination cost persists. V^* is an extension of EHI.

5.16.6 Institutional Stability Threshold

Institutional stability exists when:

$$V_{total} < V_{crit}$$

If exceeded, adaptive responses include:

- expansion of regulation
- administrative growth
- increased monitoring and enforcement
- intensified buffering

These responses increase systemic energy expenditure. Stability depends on whether society can keep up with its own diversity.

5.16.7 Energetic Limits of High-Coordination Systems

Institutional systems operate under energetic constraint:

$$E_{total} \leq E_{capacity}$$

If assimilation load approaches capacity:

- institutional efficiency declines
- coordination cost rises nonlinearly
- buffering becomes less effective
- structural adaptation becomes necessary.

5.16.8 Sensitivity of High-Trust Societies

High-trust, low-variance systems display nonlinear sensitivity to variance increases. Even modest variance differentials may generate:

- regulatory expansion
- institutional layering
- increased administrative mediation

These are structural coordination responses rather than normative judgments.

5.16.9 Selection Mismatch and Ecological Transition

When populations shaped under different ecological constraint regimes interact within a single institutional system, temporary mismatch may arise. This increases coordination load until convergence or institutional adaptation reduces variance differential.

5.16.10 Empirical Institutional Indicators (Denmark)

Energetic cost manifests through institutional indicators:

- labor-market integration lag
- welfare buffering intensity
- administrative expansion
- legal and regulatory load
- educational adaptation cost

These represent fiscal expressions of deeper coordination-variance dynamics.

5.17 Danish fiscal profiles

Fiscal transfers in high-capacity welfare systems can be interpreted as observable budgetary manifestations of underlying coordination load.

5.17.1 Budget flow

The Danish fiscal profiles illustrate how observable budget flows reflect deeper coordination dynamics within a high-capacity institutional system.

Table 17. Standard lifecycle fiscal patterns for native Danes and selected immigrant groups (Danish Finance Ministry, 2021).

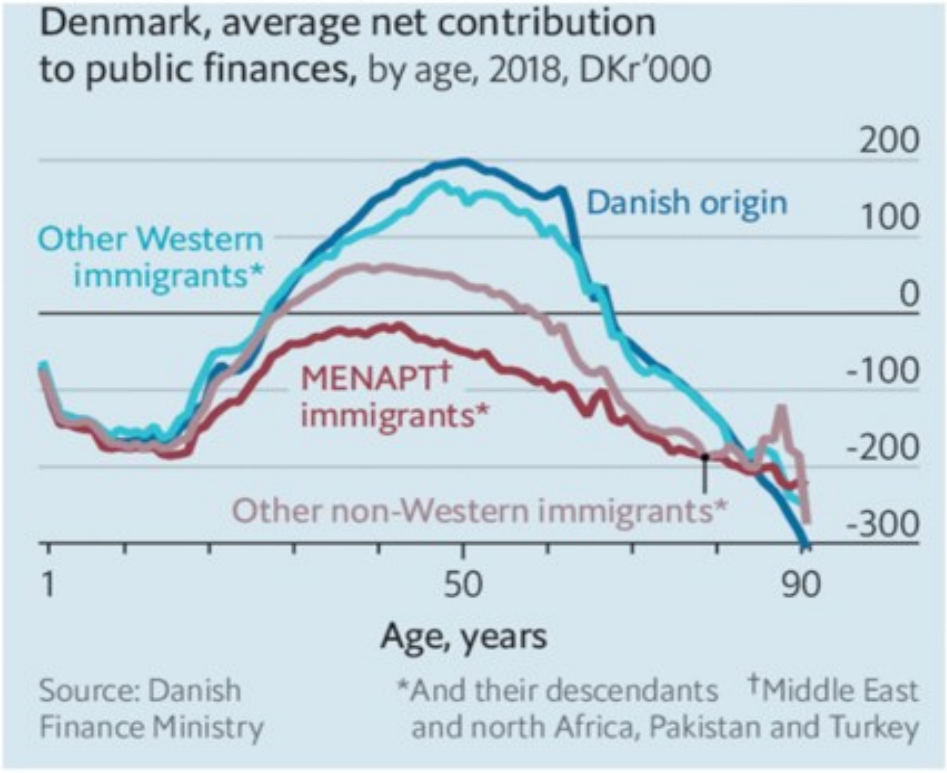

Individuals of Danish origin and Western immigrants display the standard lifecycle fiscal pattern typical of advanced welfare states: negative contributions in youth, strong positive contributions during prime working ages, and modest withdrawals in old age. In contrast, the non-Western and MENAPT curves remain substantially negative over much of the lifecycle, indicating persistent net transfers from the public budget.

Within the MESTR framework, fiscal transfers of this kind are surface expressions of underlying coordination load. High-trust welfare systems operate through dense institutional coordination—tax compliance, labor-market integration, education systems, and administrative mediation. When groups enter the system with different variance structures in human capital, employment, or institutional familiarity, the state compensates through redistribution, integration programs, and buffering mechanisms. The resulting fiscal transfers therefore represent the observable financial manifestation of deeper energetic and institutional coordination costs required to maintain systemic stability.

In MESTR terms, the fiscal deficits shown for non-Western/MENAPT groups can be interpreted as a budgetary proxy for elevated coordination cost, consistent with

$$C_c = \gamma\, V/K$$

When coordination-relevant variance V (in skills, employment stability, institutional familiarity, or norms affecting compliance) rises faster than coordination capacity K can absorb it, the welfare state must increase

buffering and administrative mediation, and the resulting net transfers become the observable fiscal footprint of that deeper coordination load.

5.17.2 MESTR–EHI Integration

Ecological constraint historically compressed variance. Modern buffering reduces environmental constraint but does not immediately alter inherited variance structure, producing temporary energetic imbalance during assimilation.

5.17.3 Long-Run Structural Outcome

Assimilation outcome depends on four parameters:

- variance differential
- buffering elasticity
- convergence rate
- institutional capacity

Different parameter regimes produce:

- full convergence and normalization
- persistent elevated coordination load
- structural institutional adaptation

5.17.4 Generalized Systems Interpretation

Assimilation is fundamentally a variance–energy allocation problem within a bounded institutional system. Fiscal expenditure is a surface expression of deeper coordination dynamics governed by MESTR energetic constraints.

5.17.5 Conclusion

The Danish case illustrates that in high-coordination institutional systems, assimilation cost is primarily an energetic coordination phenomenon rather than purely fiscal.

Institutional stability depends on the balance between variance differential, buffering capacity, convergence dynamics, and systemic energetic limits.

5.18 Variance & Institutional Dynamics

5.18.1 Variance structure and Coordination

A persistent problem in evolutionary and social science is to explain why complex cognitive capacities and large-scale institutions emerged unevenly across human populations despite a common species origin. Classical evolutionary theory emphasized competition, adaptation, and resource constraints, while modern approaches increasingly recognize the central role of energy flows in shaping biological and social systems.

The MESTR framework conceptualizes recent human evolution as a response to systematic changes in available energy induced by latitudinal migration. Declining solar irradiation, increased seasonality, and reduced primary productivity imposed strong selection pressures on metabolism, cognition, and social organization. Energy availability alone cannot explain variation in long-run outcomes. The efficiency with which populations coordinate, cooperate, and transmit information determines how much of the available energy can be converted into adaptive traits and institutions.

Two factors are critical in this regard: genetic diversity and assimilation. These concepts are often treated normatively in contemporary discourse but have clear energetic interpretations. This part of the study reformulates them within the MESTR framework and examines their consequences for population-level adaptation under ecological constraint.

5.18.2 Testable implications of the MESTR–assimilation framework

The MESTR framework, augmented with genetic diversity and assimilation as coordination parameters, yields several empirically testable predictions:

These predictions distinguish the MESTR–assimilation framework from models that treat diversity as uniformly beneficial or that rely exclusively on direct genetic causation.

Assimilation is often treated normatively in social science. Within MESTR, it is better understood as an energetic optimization process. Assimilation increases predictability of behavior, reliability of norms, efficiency of communication, and fidelity of cultural transmission.

Thus, under MESTR, assimilation is selected for in harsh environments; not because of ideology or preference, but because heterogeneity increases coordination costs that harsh ecologies cannot easily absorb.

Assimilation reduces heterogeneity in behavioral norms, cognitive styles, and social expectations. Within MESTR, assimilation is not a cultural preference but an energetic optimization. By reducing variance, assimilation lowers the energetic and informational costs of maintaining social cohesion (Pontzer,

2017). Selection therefore favors stronger assimilation pressures in environments where surplus energy is limited and coordination failures are costly.

5.18.3 Genetic Diversity and Coordination Costs

Genetic diversity increases variance in physiology, development, and behavior. While diversity can be advantageous in fluctuating environments, it also raises coordination costs in tightly coupled social systems. Greater heterogeneity increases the energetic expenditure required for communication, norm enforcement, trust formation, and collective action. These costs are often negligible in energy-rich environments but become salient under sustained scarcity.

5.18.4 Ecozone discontinuities

Differences in cognitive and institutional outcomes should cluster by ecological regime (ecozone) rather than vary smoothly with latitude alone, reflecting threshold effects in coordination efficiency.

5.18.5 Assimilation as an Energetic Process

The association between genetic similarity, assimilation, and cognitive or institutional outcomes should strengthen monotonically with increasing environmental harshness (e.g., seasonality, winter length, reduced net primary productivity (NPP) and weaken in energy-rich environments.

5.18.6 Coordination-cost scaling

In populations with high genetic and cultural heterogeneity, the energetic cost of maintaining institutional complexity should scale superlinearly with population size, particularly in harsh environments.

5.18.7 Mediation by assimilation

The relationship between environmental harshness and long-run outcomes should be partially mediated by measures of social and cultural assimilation, rather than being fully explained by ecology or genetics alone.

5.19 Energetic Constraint, Variance Dynamics, and Institutional Stability

5.19.1 Introduction

This chapter extends the MESTR framework by integrating ecological constraint, demographic transition, and institutional stability into a unified energetic–demographic model. The focus is structural: how long-run ecological environments influence variance, selection gradients, and institutional coordination, and how these relationships transform under technological buffering and demographic mobility.

The analysis does not assume intrinsic biological differences between human populations. Instead, it examines how ecological and demographic processes shape variance and coordination across time, and how institutional systems respond to changing constraint regimes.

5.19.2 Ecological Constraint and Energetic Filtering

Ecological harshness historically structured survival conditions by imposing energetic demands associated with seasonality, thermoregulation, storage, and coordination. Under persistent constraint, survival favored behavioral strategies compatible with long-range planning, delayed reward, and

cooperative organization. Within MESTR, this process is termed energetic filtering.

Over extended time horizons, ecological filtering may influence demographic composition through differential survival and fertility, as well as institutional reinforcement of adaptive behaviors. Following Lotka (1922), long-run system persistence is governed by effective energy throughput. In Odum's (1995) system perspective, stability depends on balanced energy allocation within bounded capacity. Smil (2004) anchors long-run energy availability and institutional complexity growth. These processes are conditional and environment-dependent rather than deterministic.

We operationalize ecological constraint through the EHI, providing a standardized measure of the energetic burden imposed by environmental volatility (conf. Part III).

5.19.3 Historical Selection and Institutional Continuity

Pre-industrial demographic regimes may have exhibited directional selection associated with socioeconomic stratification, urbanization, and diffusion of behavioral norms (Clark, 2007). Within MESTR, such processes are interpreted as selection operating under persistent ecological constraint and institutional continuity.

The emphasis remains structural. Ecological regimes shape selection gradients, but these gradients transform when environmental and technological conditions change.

5.19.4 Technological Buffering and Transformation of Selection Gradients

Industrialization altered ecological constraint through technological buffering, reducing mortality risks and stabilizing resource availability. Selection persists, but its gradient transforms.

Let:

EHI = ecological harshness

T = technological buffering

S = selection gradient

Then:

$$S \propto (EHI - T)$$

As technological buffering increases, energetic filtering weakens and variance in behaviorally relevant traits may expand (Pontzer, 2017). This transformation reflects a shift in selection structure rather than a reversal of Darwinian processes.

5.19.5 Transitional Dynamics Under Rapid Demographic Change

Rapid demographic change may generate transitional challenges driven by variance and coordination dynamics.

5.19.6 Institutional Adaptation

Institutional stability depends, as shown previously, on the rate of demographic change relative to institutional adaptation. Historical transitions often involve temporary instability followed by new equilibria.

Energetic–Demographic Formalization:

Selection gradient

$$S \propto EHI - T$$

S is normalized such that S = $k(EHI - T)$, k > 0

The previously defined variance dynamics:

$$\frac{dV}{dt} = -\alpha(EHI - T)\,V + \beta T\left(1 - \frac{V}{K}\right)$$

$$I \propto \frac{1}{V}$$

5.19.7 Integration with MESTR and EHI

The MESTR framework links ecological constraint, demographic transition, and institutional performance through energetic filtering and variance dynamics. Assimilation across ecological histories is thus interpreted as a dynamic process shaped by:

- Ecological constraint (EHI)
- Selection gradient transformation
- Variance dynamics
- Institutional adaptation.

5.19.8 Effective Ecological Constraint

Let:

EHI = ecological harshness

T = technological buffering

define effective constraint:

$$E^* = EHI - T$$

Effective constraint E^* represents Ecological Harshness moderated by technological buffering, an extension of EHI.

This distinguishes geographic environmental burden from technologically mediated survival conditions.

5.19.9 Transformation of Selection Gradients

Selection persists under all ecological regimes, but its gradient varies with effective constraint:

$$S \propto E^*$$

When $E^* > 0$, ecological filtering is strong and variance tends to compress. When $E^* \approx 0$, filtering weakens and variance may expand.

This represents, as said, a transformation of selection structure rather than a reversal of energetic processes.

- Strong ecological constraint compresses variance.
- Strong buffering expands variance.

Variance dynamics form the direct link between ecological constraint and institutional coordination.

5.19.10 Institutional Stability and Coordination Cost

Institutional stability is inversely related to coordination-relevant variance:

$$I \propto \frac{1}{V}$$

When demographic variance expands faster than institutions adapt, coordination cost and institutional load increase temporarily until a new equilibrium emerges.

5.19.11 Demographic Assimilation as Structural Convergence

Assimilation is modelled as convergence toward institutional equilibrium:

$$V_{total(t)} \rightarrow V_{eq}$$

The rate depends on:

- Educational integration
- Intergenerational transmission
- Institutional adaptation speed

This is a structural demographic process rather than a statement about inherent population traits.

5.19.12 Transitional Dynamics

Rapid demographic transition may temporarily increase:

- Variance
- Coordination cost
- Institutional load

Historical demographic systems repeatedly exhibit such transitional instability before stabilization.

5.19.13 Synthesis

Ecological constraint, demographic structure, and institutional continuity jointly shape long-run variance and coordination. Technological buffering transforms these relationships by weakening ecological filtering and altering selection gradients. Assimilation is therefore a dynamic structural process governed by energetic constraint, demographic variance, and institutional adaptation.

Historical clustering of accomplishment and transitional challenges under demographic change can be understood within a unified ecological–demographic framework. The key mechanism is the interaction among ecological constraint, energetic filtering, demographic variance, and institutional stability.

5.20 Macro-energetic and Growth Implications

A unified interpretation of long-run human development emerges when the energetic logic of MESTR is combined with the macro-historical transition described in Unified Growth Theory (UGT; Oded Galor, 2011, 2022). The two frameworks operate at different analytical levels but address the same fundamental process: how ecological constraint, demographic structure, and human capital co-evolve over time to produce the transition from subsistence-bound systems to sustained growth.

5.20.1 Energetic constraint as the deep initial condition

In the MESTR framework, Environmental Harshness (EHI) defines the thermodynamic constraint surface governing the balance between usable

ecological energy and the metabolic cost of survival, regulation, and coordination. Where energetic constraint is high, selection favors strategies that increase efficiency, planning depth, and coordination stability while narrowing admissible variance through energetic filtering, truncation selection, and canalization. This relationship constitutes a variance law of environmental constraint, formalized as:

$$Var(Y) = \alpha - \beta_1 EHI - \beta_2 Var(EHI), \beta_1, \beta_2 > 0$$

where increasing ecological constraint and environmental volatility compress outcome variance. Over long timescales, this variance compression stabilizes behavioral and institutional coordination, enabling reliable transmission of skills, norms, and intergenerational investment.

From a thermodynamic perspective, biological and social systems can be understood as dissipative structures maintaining organization through energy throughput. Within this framework, MESTR describes how environmental constraint shapes the admissible configuration space of such systems, with selection favoring energetically efficient and stable coordination regimes. This interpretation extends classical energetic principles to institutional and macro-social domains.

5.20.2 The Malthusian regime as an energetic–demographic equilibrium

Unified Growth Theory (Galor, 2011, 2022) describes the pre-modern world as a Malthusian regime in which technological or productivity gains are largely absorbed by population growth, leaving per-capita income near subsistence. Within the integrated interpretation, this regime corresponds to

a state where ecological constraint and demographic feedback maintain a dynamic energetic equilibrium:

- Ecological energy sets the ceiling for surplus.
- Surplus regulates population density.
- Population pressure feeds back into resource competition.

MESTR provides the micro-foundational layer of this equilibrium. Under persistent constraint, selection gradually alters life-history timing, cooperation, and cognitive investment, while founder effects and truncation selection reduce variance. These processes do not immediately produce growth but restructure the population's adaptive capacity, laying the groundwork for later transitions.

5.20.3 Transition to post-Malthusian dynamics: variance and human capital

UGT identifies the demographic transition and rising human capital investment as the key mechanism enabling escape from the Malthusian trap. In the MESTR framework, this transition is interpretable as a variance–energy phase shift.

As coordination efficiency increases and variance declines, systems become capable of sustaining:

- longer planning horizons,
- greater intergenerational investment,
- stable institutional memory,
- reliable transmission of knowledge.

This allows a shift from quantity-maximizing reproduction toward quality-oriented human capital accumulation. The demographic transition—declining fertility and increasing parental investment—thus reflects a change in energetic allocation under stabilized variance rather than a purely cultural or technological break.

In this integrated model:

- EHI shapes the initial constraint and variance structure,
- MESTR selection gradually stabilizes coordination and human capital potential,
- UGT describes the macro-level transition once human capital accumulation becomes self-reinforcing.

5.20.4 Sustained growth as an emergent coordination regime

In the final stage of UGT, sustained economic growth emerges through technological innovation, knowledge accumulation, and demographic stabilization. From the MESTR perspective, this phase represents a regime in which coordination capacity and institutional buffering allow systems to maintain high energetic throughput without destabilizing variance expansion.

Growth therefore depends on three interacting layers:

1. Energetic layer (MESTR) — defines constraint surface and variance regulation.

2. Demographic–human capital layer (UGT) — reallocates energy from population growth to knowledge and skill.

3. Institutional–coordination layer (MESTR extension) — stabilizes large-scale cooperation and enables cumulative innovation.

Technological progress alone cannot explain sustained growth. It must operate within a population and institutional structure capable of managing energetic and variance constraints.

5.20.5 Thermodynamic continuity across regimes

This synthesis reveals continuity rather than discontinuity between energetic adaptation and modern growth. The same energetic principles govern all phases:

- Under high constraint: variance compression and robustness selection dominate.
- During transition: coordination stabilizes and human capital accumulates.
- In sustained growth: energetic throughput increases under buffered variance.

Thus, MESTR provides the deep energetic and thermodynamic substrate, while UGT describes the emergent macro-historical trajectory. Together they form a continuous account linking ecological constraint, variance dynamics, demographic transition, institutional coordination, and long-run economic growth.

5.21 Formal Integration of MESTR and Unified Growth Theory (UGT)

MESTR provides, in other words, the energetic micro-foundation of the macro-historical transition described in Unified Growth Theory (UGT; Galor, 2011, 2022):

Energetic Constraint → Variance Regulation → Human Capital → Sustained Growth.

5.21.1 Energetic Constraint Field (MESTR foundation)

Let ecological harshness E (EHI) define the thermodynamic constraint on usable energetic surplus:

$$S = E_u - C_m$$

where

E_u = usable environmental energy,

C_m = metabolic survival and regulation cost,

S = surplus available for growth, buffering, neural investment, and coordination.

Higher $E \Rightarrow$ lower $S \Rightarrow$ tighter allocation and stronger selection for efficiency and robustness.

Selection operates on energetic viability, not only trait means. Under persistent constraint:

- developmental latitude narrows,
- truncation selection removes low-robustness variants,
- phenotypic and institutional variance compress.

This yields the previously mentioned MESTR variance law:

$$\mathrm{Var}(Y) = \alpha - \beta_1 EHI - \beta_2 \mathrm{Var}(EHI), \beta_1, \beta_2 > 0$$

Outcome variance declines as constraint and environmental volatility increase.

5.21.2 Demographic–Energetic Equilibrium (Malthusian regime)

Let population size be N, fertility f, mortality d, and carrying capacity determined by energetic surplus:

$$\dot{N} = N(f(S) - d(S))$$

In the Malthusian regime:

1. productivity gains raise S,
2. higher S increases N,
3. rising N reduces per-capita surplus,
4. system returns to subsistence equilibrium.

Thus ecological constraint and demographic feedback produce a stable energetic equilibrium.

MESTR adds micro-foundations: under persistent constraint, selection gradually modifies life-history timing, cooperation, and cognitive investment while compressing variance, increasing system robustness without yet generating sustained growth.

5.21.3 Variance–Coordination Phase Transition

Let coordination efficiency be K, institutional buffering capacity B, and coordination-relevant variance V.

Institutional stability requires:

$$K \geq V$$

Coordination cost:

$$C_c = \gamma \frac{V}{K}$$

Assimilation / variance inflow V_{in} evolves as:

$$\dot{V} = V_{in} - \lambda V$$

where λ = convergence rate (integration, learning, institutional adaptation).

Under MESTR selection:

- long-run V declines,
- K rises (cooperation, planning, norm reliability),
- coordination cost falls,
- buffering becomes more efficient.

This produces a variance-stabilized regime, enabling long planning horizons and intergenerational investment.

5.21.4 Human Capital Transition (UGT linkage)

Let human capital be H, fertility f, and investment share in offspring q.

Energetic allocation constraint:

$$S = C_m + C_c + C_r + C_h$$

where

C_r= reproductive quantity cost,

C_h= human capital investment.

As variance stabilizes and coordination becomes reliable:

$$\frac{\partial H}{\partial K} > 0, \frac{\partial f}{\partial H} < 0$$

The system shifts from quantity-maximizing reproduction to quality-maximizing investment:

$$f \downarrow, H \uparrow \text{,planning horizon} \uparrow$$

This is the demographic transition described in Unified Growth Theory.

5.21.5 Emergence of Sustained Growth

Output per capita depends on human capital, coordination efficiency, and technology A:

$$y = A \cdot F(H, K)$$

Knowledge accumulation:

$$\dot{A} = \phi HK$$

Sustained growth requires:

$$\dot{A} > \delta$$

where δ = dissipation / depreciation.

In the integrated model:

- MESTR determines initial constraint and variance structure,
- variance compression increases coordination stability,
- stable coordination enables human capital accumulation,
- human capital drives technological growth,
- technological growth increases energetic throughput without destabilizing variance.

Thus sustained growth is a stable high-throughput energetic regime, not merely technological acceleration.

5.21.6 Regime Structure

Table 18. Regime Structures and outcomes.

Regime	Energetic Condition	Variance	Demography	Growth
Malthusian	High constraint	High	High fertility	No sustained growth
Transition	Constraint + stabilization	Falling	Falling fertility	Slow growth
Sustained growth	Buffered constraint	Low, stable	Low fertility	Continuous growth

5.21.7 Thermodynamic Continuity

Across all regimes, the governing principle is energetic:

- Systems persist far from equilibrium by dissipating energy gradients.
- Selection favors energetically viable and variance-stable configurations.
- Growth emerges when coordination, human capital, and energetic throughput align.

Thus: MESTR = energetic–variance micro-foundation; UGT = macro-historical growth trajectory.

Together they form a continuous theory linking ecological constraint, energetic adaptation, demographic transition, institutional coordination, and long-run economic growth.

5.22 Model Summary and Testable Predictions

5.22.1 Thermodynamic Foundations of Energetic Constraint

The energetic perspective adopted in this volume is, as expected under the model, consistent with the non-equilibrium thermodynamic view of organized systems originally articulated by Boltzmann (1974). Complex adaptive systems—including biological populations and institutional structures—maintain order by dissipating energy gradients. Stability therefore depends not only on structural configuration but on the continuous availability and allocation of usable energy.

Within the present framework, ecological constraint historically regulated the energetic environment under which coordination, planning, and institutional reliability evolved. Modern technological and institutional buffering modifies direct environmental pressure but does not remove the underlying energetic condition: coordination and institutional stability require sustained energetic throughput.

Assimilation, in this perspective, represents a redistribution of coordination energy within a bounded system. Increased variance raises the energetic cost of maintaining institutional order, requiring additional buffering, regulation, and administrative effort. These adjustments reflect the thermodynamic principle that maintaining structured organization under changing conditions requires increased energy dissipation (Boltzmann, 1974).

Thus, the MESTR model is fundamentally an energetic systems framework: institutional stability, variance dynamics, and buffering capacity are constrained by the allocation and limits of systemic energy.

The present model extends the thermodynamic–energetic lineage from Boltzmann through Lotka and Odum into an institutional variance framework, going from thermodynamic constraint (Boltzmann) → Energetic selection (Lotka) → System energy allocation (Odum) → Historical energy–institution link (Smil) to the MESTR variance–institution model.

5.22.2 Core Structure of the Energetic–Institutional Model

The present framework integrates ecological constraint, variance dynamics, and institutional stability within this unified energetic perspective. The model

treats assimilation as a coordination and buffering process operating inside a bounded institutional energy system.

Let ecological harshness be represented by the Environmental Harshness Index (EHI), and technological–institutional buffering by T. Technological buffering reduces effective ecological constraint, producing

$$E^* = EHI - T$$

where T represents institutional and technological buffering capacity.

Higher effective constraint historically compresses variance and strengthens coordination efficiency, whereas buffering reduces direct ecological pressure but does not immediately eliminate inherited variance structure.

Institutionally relevant variance is decomposed as:

$$V_{total} = V_H + V_I + V_{between}$$

where V_H denotes variance within the host population, V_I variance within the incoming population, and $V_{between}$ the variance between institutional–behavioral distributions of the two. Assimilation primarily operates through changes in $V_{between}$.

Coordination cost increases approximately proportionally to inter-group variance:

$$C_{coord} = \alpha V_{between}$$

Institutional stability is inversely related to coordination-relevant variance:

$$I \propto \frac{1}{V_{total}}$$

Thus, increases in total variance raise coordination cost and reduce institutional stability unless offset by buffering or convergence.

The dynamic component of assimilation is represented by:

$$\frac{dV_{between}}{dt} = -\lambda V_{between} + \delta$$

where λ is the convergence (integration) rate and δ represents structural variance inflow. The long-run equilibrium variance is:

$$V^*_{between} = \frac{\delta}{\lambda}$$

Institutional systems operate under energetic constraint; total coordination and buffering effort cannot exceed systemic capacity. When variance rises beyond the adaptive range of institutional buffering, administrative expansion and regulatory growth occur as compensatory responses.

5.23 Interpretation: General Perspective

Within this framework, assimilation is not primarily a fiscal process but a variance–coordination–buffering interaction within a bounded institutional energy system. Fiscal expenditures represent observable manifestations of deeper coordination and buffering dynamics.

Short-run effects of assimilation include increased coordination load and expanded buffering. Long-run outcomes depend on the relative magnitude of variance inflow and convergence rate. Where convergence dominates, institutional load declines; where variance persists, structural adaptation occurs.

High-coordination institutional systems characterized by historically low variance exhibit nonlinear sensitivity to increases in $V_{between}$, implying that marginal coordination cost may rise faster than variance itself.

Testable Predictions:

The MESTR framework generates a series of empirical predictions linking ecological constraint, variance structure, institutional coordination, and long-run development. These predictions follow directly from the energetic–variance relationships described in the model.

5,23.1 Variance Law of Environmental Constraint

Outcome variance in coordination-relevant traits should decline with increasing ecological constraint:

$$Var(Y) = \alpha - \beta_1 EHI - \beta_2 Var(EHI)$$

Prediction:

Regions with higher environmental harshness (high EHI) will exhibit lower variance in coordination-relevant outcomes such as educational attainment, institutional reliability, and labor-market participation.

5.23.2 Environmental Volatility and Institutional Stability

Environmental volatility increases coordination demands.

Prediction:

Regions with greater climatic volatility will display stronger institutional stabilization mechanisms, including rule enforcement, social insurance systems, and long planning horizons.

5.23.3 Energetic Constraint and Cooperation

Under persistent ecological constraint, selection favors cooperation and coordination efficiency.

Prediction:

Populations historically exposed to higher energetic constraint should display higher levels of social coordination capacity, including institutional trust, rule adherence, and long-term planning.

5.23.4 Technological Buffering and Variance Expansion

Technological buffering reduces effective ecological constraint:

$$E^* = EHI - T$$

Prediction:

As technological buffering increases, the variance-compressing effect of ecological constraint should weaken, producing greater dispersion in outcomes and behavioral strategies**.**

5.23.5 Coordination Load and Fiscal Transfers

Institutional coordination requires energetic and administrative resources.

$$C_c = \gamma \frac{V}{K}$$

Prediction:

When coordination-relevant variance V exceeds institutional coordination capacity K, welfare states will exhibit higher fiscal transfers, integration expenditures, and administrative mediation, reflecting increased coordination load.

5.23.6 Demographic Transition and Human Capital

Variance stabilization and coordination reliability enable long-term investments in offspring quality.

Prediction:

Regions with stable coordination systems should display lower fertility and higher human capital investment**,** as predicted under the model, consistent with the demographic transition described in Unified Growth Theory.

5.23.7 Long-Run Growth Dynamics

Sustained growth requires stable coordination and human capital accumulation.

$$y = A \cdot F(H, K)$$

Prediction:

Societies combining high coordination capacity K with high human capital H will sustain long-run technological growth, whereas societies with high variance and weak coordination will remain trapped in low-growth equilibria.

5.23.8 Summary

Because these predictions are directly testable using ecological, demographic, institutional, and economic data, the framework provides a falsifiable energetic foundation for the study of long-run development.

5.23.9 Concluding Note

The energetic–institutional model provides a formal but parsimonious framework linking ecological constraint, demographic integration, and institutional stability. It emphasizes dynamic interaction rather than static outcomes and identifies variance, buffering capacity, and convergence rate as the key determinants of long-run systemic equilibrium.

5.24 A Thermodynamic Interpretation of Environmental Adaptation

At the largest scale, life can be understood as a dissipative structure embedded in planetary energy flow (Schrödinger, 1944; Prigogine & Stengers, 1984). Evolution reflects the progressive optimization of energy capture, allocation,

and stability under shifting environmental constraints. Within this cosmo-physical interpretation:

- EHI defines the local thermodynamic constraint field, and
- MESTR defines the energetic response function mapping energetic constraint to biological strategy.

Together they connect solar forcing, ecological productivity, metabolic allocation, neural investment, and behavioral complexity into a unified physical account of environmental adaptation.

Future work formalizes this relationship by quantifying energetic surplus, coordination cost, and stability optimization across environmental gradients, thereby linking ecological energetics to the broader trajectory of organismal and systemic complexity within planetary energy flow.

Figure 4: The Master framework of the Migration–Energetic Selection and Trade-off (MESTR) model (Author-generated schematics).

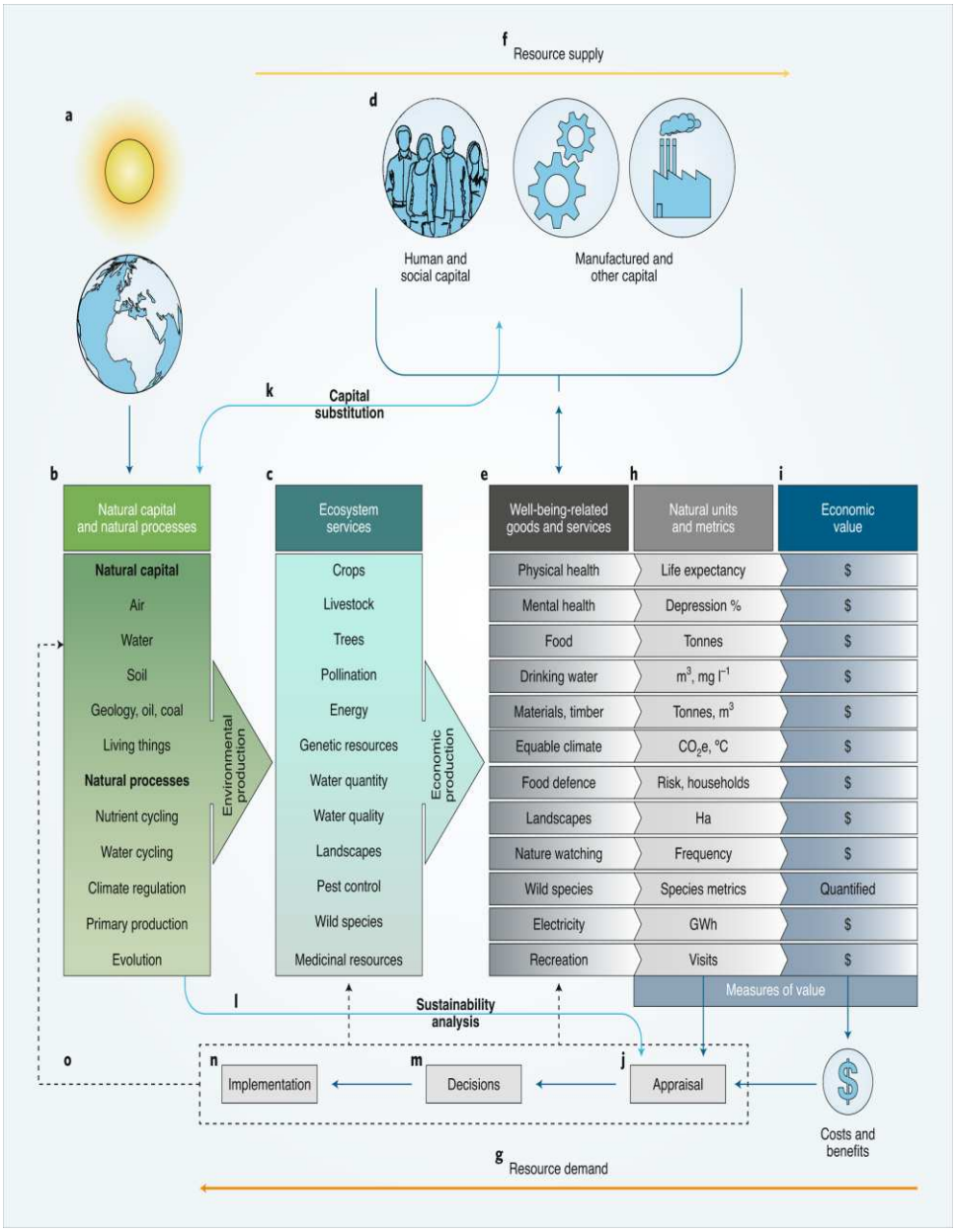

Here ecological constraint shapes energetic trade-offs that regulate variance in coordination-relevant traits. Stabilized variance enables institutional coordination and human capital accumulation, ultimately supporting sustained technological and economic growth. Technological buffering reduces effective constraint but does not eliminate the underlying energetic structure.

5.25 Life as a non-equilibrium energetic process

All living systems persist far from thermodynamic equilibrium and require continuous throughput of free energy to maintain structure, repair damage, and reproduce. The biosphere is an open, solar-driven dissipative system in which biological organization emerges through the capture, transformation, and dissipation of environmental energy gradients. Evolution therefore operates under energetic constraint: selection favors phenotypes that optimize energy acquisition, allocation, and stability within locally imposed physical limits (Lotka, 1922; Schrödinger, 1944; Odum, 1995).

From an energetic perspective, environmental variation represents variation in thermodynamic boundary conditions governing biological viability.

5.26 Unified Conclusion

5.26.1 Energetic Constraint, Variance Dynamics, Institutional Stability, and Limitations

The present volume has developed a unified framework linking ecological constraint, energetic allocation, variance structure, and institutional stability within the broader MESTR model. Across energetic and historical time, ecological harshness shapes the distribution of behaviorally and institutionally relevant traits, influencing coordination efficiency and long-run social organization.

Institutional stability emerges from the interaction between variance and coordination capacity. When variance remains within the adaptive range of institutional buffering, systems maintain efficient operation. When variance expands beyond buffering capacity, coordination costs rise and institutional adaptation becomes necessary. This relationship is captured formally by the inverse relation between institutional stability and coordination-relevant variance.

Assimilation represents a dynamic case of variance interaction within a bounded institutional energy system. The analysis has shown that assimilation cost is fundamentally energetic rather than purely fiscal. Coordination load, buffering expenditure, and administrative adaptation together determine the systemic burden imposed by variance differential. Fiscal transfers are therefore surface manifestations of deeper energetic coordination dynamics.

The Danish case has illustrated how high-coordination, low-variance institutional systems respond to variance increases through buffering

expansion and administrative adaptation. The magnitude and persistence of energetic cost depend on the balance between variance differential, convergence dynamics, buffering elasticity, and institutional capacity. Where convergence dominates, coordination load declines over time; where variance persists, institutional adaptation becomes structural.

Within the EHI–MESTR framework, ecological constraint historically compressed variance, while modern technological and institutional buffering reduce environmental constraint without immediately altering inherited variance structure. Assimilation therefore temporarily increases energetic imbalance until convergence or structural adaptation restores equilibrium.

The broader implication is that institutional systems operate under energetic limits. Stability is maintained not by eliminating variance, but by balancing variance against buffering capacity and coordination efficiency. This perspective provides a unified interpretation of ecological constraint, demographic integration, and institutional dynamics across historical and contemporary contexts.

Future research may refine the quantitative mapping between variance structure, energetic allocation, and institutional outcomes, extending the present framework across ecozones and historical transitions. The MESTR model thus offers a general systems approach to understanding the energetic foundations of social organization and long-run institutional stability.

5.26.2 Limitations

Several limitations warrant explicit acknowledgment. First, all analyses operate at the population level using national or regional aggregates. The framework does not make claims about individual traits, abilities, or outcomes, and ecological correlations must not be interpreted as individual-level determinism. Second, genetic distance and diversity measures are proxies that capture historical population structure rather than specific functional genetic mechanisms. Third, ecozones and national boundaries remain coarse spatial units that obscure substantial within-region heterogeneity.

In addition, assimilation and coordination costs are inferred rather than directly measured. While energetic and institutional inefficiencies are well-established consequences of heterogeneity in complex systems, future work would benefit from direct indicators of coordination expenditure, institutional overhead, and social friction. Finally, the framework is explicitly conditional: in energy-rich or technologically buffered environments, the selective pressure favoring assimilation is expected to weaken, and diversity may become neutral or advantageous.

These limitations do not undermine the descriptive patterns documented here, but they constrain causal interpretation and define the scope of valid inference.

5.27 Likely objections

To consider likely objections to the fundamental observation of variance inversion under MESTR, we line up several possible scenarios and detail responses.

> "The variance inversion may be a statistical artifact of aggregation or unequal sample sizes."

A common concern is that reduced outcome variance in high-latitude ecozones could reflect aggregation bias, ceiling effects, or smaller effective sample sizes rather than energetic processes. Several features of the present design mitigate this concern.

First, the variance inversion is observed across multiple, conceptually independent outcome domains—including cranial capacity, cognitive performance, fertility, androgen receptor variation, and institutional indicators—measured using different data sources and historical periods. It is therefore unlikely to arise from a single measurement artifact.

Second, ecozone groupings were defined independently of outcome variables, based solely on latitude and environmental inputs. Variance differences thus emerge as empirical consequences rather than imposed constraints.

Third, the same mirror pattern is evident when outcomes are treated continuously (EHI-based analyses) and when they are discretized into ecozones, reducing the likelihood that it is driven by group size or discretization alone.

Finally, the prediction that outcome variance should decline as environmental variance increases is not ad hoc but follows directly from established results in quantitative genetics and truncation selection theory (Fisher, 1930; Falconer & Mackay, 1996).

> "If environments are more variable, why would outcomes become more homogeneous?"

This objection implicitly assumes that environmental variance is transmitted linearly into phenotypic variance. That assumption does not hold under sustained energetic constraint.

In the MESTR framework, increasing variance in energetic inputs raises the cost of failure and therefore narrows the range of viable phenotypic and institutional strategies. Systems that function only under favorable conditions are eliminated, while those that perform robustly across fluctuations persist. This is the classical logic of canalization (Waddington, 1957): phenotypic variance is reduced precisely because environmental variance is high.

Thus, the observed variance inversion is not paradoxical but diagnostic of long-term selection for robustness under volatile energetic regimes.

> "Founder effects alone cannot explain systematic reductions in outcome variance."

Founder effects alone are insufficient, and this limitation is explicitly acknowledged. Within MESTR, founder effects operate as an initial variance filter, reducing standing genetic and phenotypic diversity along the migration axis. However, the sustained reduction of outcome variance in high-EHI

ecozones requires directional and truncation selection operating over many generations.

The key claim is therefore not that founder effects explain the variance inversion, but that founder effects and truncation selection act multiplicatively. Founder effects reduce the raw material on which selection acts; truncation selection then removes remaining low-robustness variants. This combined process is well established in evolutionary genetics and produces rapid variance collapse even when means shift gradually.

> "Could cultural or institutional homogenization, rather than biological selection, explain the pattern?"

Cultural and institutional processes undoubtedly contribute to outcome variance, particularly for societal indicators. However, several considerations argue against a purely cultural explanation.

First, the variance inversion is observed not only for institutional outcomes but also for biological traits such as cranial capacity, stature, fertility timing, and androgen receptor polymorphism, which are not plausibly homogenized by modern institutions.

Second, institutional homogenization itself requires explanation. In MESTR terms, high-EHI environments impose energetic and coordination demands that favor low variance in cooperation, rule compliance, and long-term planning. Cultural canalization is therefore interpreted as a downstream expression of the same energetic constraints, not as an alternative mechanism.

Thus, biological and cultural processes are treated as complementary channels through which energetic selection operates, rather than competing explanations.

> "Does this imply environmental or genetic determinism?"

No.

All analyses are conducted at the population and ecozone level and describe long-term statistical regularities, not individual outcomes. High-EHI environments constrain the distribution of viable strategies but do not uniquely determine any individual's phenotype, cognition, or life trajectory.

Moreover, the presence of substantial between-ecozone mean differences alongside reduced within-ecozone variance underscores the role of historical contingency, migration history, and institutional feedback, all of which are explicitly acknowledged in the MESTR framework.

> "Why should this pattern be considered evidence for MESTR rather than a post hoc explanation?"

The variance inversion constitutes a novel, falsifiable prediction of the MESTR framework.

A naïve climate or latitude model would predict that harsher and more variable environments produce both higher means *and* higher variances in outcomes. MESTR predicts the opposite for variance: increasing environmental volatility should be associated with decreasing outcome variance due to truncation selection and canalization.

The empirical observation of this mirror pattern across multiple domains therefore strengthens, rather than weakens, the theoretical coherence of the framework.

Taken together, the mirror pattern of increasing environmental SD and decreasing outcome SD is best understood as a signature of long-term adaptation under energetic constraint. It reflects the combined action of serial founder effects, truncation selection, and canalization rather than statistical artifact, cultural homogenization, or deterministic environmental causation. Addressing this pattern explicitly clarifies why the MESTR framework predicts not only mean differences across ecozones but also systematic differences in variance structure.

APPENDICES

A: Environmental Harshness Index (EHI): Specification, Construction, and Replication

A1 Physical construction of EHI

EHI operationalizes thermodynamic constraint through physically grounded environmental variables:

A2 Solar–productive limitation

$$E_{in} \propto \text{NPP (Net Primary Productivity)}$$

Lower productivity reduces ecological energy throughput (Running et al., 2004).

A3 Thermoregulatory load

$$E_{maint} \uparrow \text{ as } T_{min} \downarrow \text{ and temperature seasonality} \uparrow$$

Lower temperatures and higher variability increase metabolic maintenance costs (Clarke & Fraser, 2004).

A4 Photoperiodic and seasonal constraint

$$E_{in,effective} \downarrow \text{ as photoperiod variability and winter duration} \uparrow$$

Energy acquisition becomes temporally restricted, increasing buffering requirements (Forsythe et al., 1995).

Together these components approximate:

$$EHI = f(\text{Low NPP, Cold Stress, Seasonal Constraint})$$

representing the net thermodynamic pressure field acting on biological systems.

A5 Conceptual Definition

The Environmental Harshness Index (EHI) is a constraint-based ecological measure that quantifies the degree to which environments limit the capture, storage, and allocation of usable energy over the annual cycle while imposing selection-relevant physiological and temporal stress.

EHI is interpreted within the MESTR framework as an operational measure of thermodynamic constraint.

A6 Scope and Interpretation

EHI is:

an ecological constraint measure

exogenous to biological and societal outcomes

non-normative (not a ranking of populations)

EHI is not:

a measure of intelligence, wealth, or institutions

a proxy for latitude

an individual-level predictor

A7 Component Architecture

EHI integrates five canonical components:

Energy limitation

Solar irradiation (LowIrradiance = −Irradiance)

Net primary productivity (LowNPP = −NPP)

Selection-relevant stressors

Minimum temperature (Tmin)

Temperature seasonality (ΔT or BIO4)

Photoperiodic hardship (winter length or daylight deficit)

All components are oriented such that:

Higher values indicate greater environmental harshness

A8 Data Sources

Typical sources include:

Solar irradiation: WHO UV database / NASA POWER

NPP: MODIS (MOD17 series)

Temperature: WorldClim v2.x (BIO4, BIO6)

Photoperiod: astronomical derivation from latitude

All sources must report:

spatial resolution

temporal coverage

units

A9 Transformation and Standardization

Orientation:

Irradiance → multiply by −1

NPP → multiply by −1

Tmin → either raw (more negative = harsher) or inverted

Standardization:

All components are transformed to z-scores:

$$Z_i = \frac{X_i - \mu_i}{\sigma_i}$$

A10 Index Construction

Canonical EHI:

$$EHI = \frac{1}{k}\sum_{i=1}^{k} Z_i$$

where k is the number of components.

Equal weighting is the default.

A10 Variants (EHI-X)

Any deviation from canonical construction must be labeled explicitly:

EHI-PCA

EHI-Disease

EHI-Paleo

All variants must report:

weights

transformations

robustness vs canonical EHI

A11 Diagnostics (Required)

component distributions

inter-component correlations

dominance checks

leave-one-out sensitivity tests

geographic gradient validation

A12 Interpretation Principles

EHI is relative to domain and period

similar EHI values may arise from different component profiles

interpretation must remain ecological, not individual-level

A13 Formal Predictions

Let:

E= long-run EHI

$Var(E)$= within-ecozone variance of EHI

Y= outcome variable

Predictions:

Mean constraint

$$E[Y] = f(EHI)$$

Environmental variance amplification

$$\frac{\partial Var(EHI)}{\partial \mid Latitude \mid} > 0$$

Variance inversion

$$\frac{\partial Var(Y)}{\partial Var(EHI)} < 0 \mid E$$

Joint variance law

$$Var(Y) = \alpha - \beta_1 EHI - \beta_2 Var(EHI)$$

A14 Permissible Uses

independent variable

moderator

ecozone stratification

mechanism testing

A15 Impermissible Uses

embedding outcomes inside EHI

normative interpretation

individual-level inference

A16 Replication Requirements

All studies must report:

spatial unit

temporal window

data sources and versions

transformations

weighting scheme

diagnostics

code or reproducible steps

A17 Photoperiod Derivation

Given latitude ϕ and day d:

$$\delta(d) \approx 0.409 \sin\left(\frac{2\pi}{365} d - 1.39\right)$$

$$\omega_s = \arccos(-\tan\phi \tan\delta)$$

$$L(d) = \frac{24}{\pi} \omega_s$$

Photoperiodic hardship is defined as:

cumulative daylight deficit, or

number of days below threshold

A18 Example Pipelines: Python

Python (CSV-based pipeline)

```
import pandas as pd

from sklearn.preprocessing import StandardScaler

# Load component data

df = pd.read_csv("ehi_components.csv")

# Orientation: higher = harsher

df["irradiance"] = -df["irradiance"] # LowIrradiance

df["npp"]  = -df["npp"]          # LowNPP

# Tmin handling (choose ONE and state it explicitly):
```

```
# Option A (recommended): keep Tmin as-is (more negative = harsher)

# Option B (alternative): invert for intuitive direction

# df["tmin"] = -df["tmin"]

components = ["irradiance", "npp", "tmin", "seasonality", "photoperiod"]

# Standardize components (z-scores)

Z = StandardScaler().fit_transform(df[components])

# Canonical equal-weight EHI

df["EHI"] = Z.mean(axis=1)

# Save results

df.to_csv("ehi_results.csv", index=False)
```

standardize components

compute mean z-score

export EHI

A19 Example Pipeline: R

identical structure using scale() and rowMeans()

R (CSV-based pipeline)

```
df <- read.csv("ehi_components.csv")

# Orientation: higher = harsher

df$irradiance <- -df$irradiance

df$npp        <- -df$npp

# Tmin handling (choose ONE and state it explicitly):

# Option A (recommended): keep Tmin as-is

# Option B (alternative): df$tmin <- -df$tmin

components <- c("irradiance", "npp", "tmin", "seasonality", "photoperiod")

# Standardize components (z-scores)

Z <- scale(df[components])

# Canonical equal-weight EHI

df$EHI <- rowMeans(Z)

write.csv(df, "ehi_results.csv", row.names = FALSE)
```

A20 Limitations

ecological inference limits

component collinearity

uncertainty in historical reconstructions

no direct measurement of technological buffering

A21 Summary

EHI provides a portable, theory-disciplined measure of thermodynamic constraint that enables:

cross-regional comparison

longitudinal analysis

falsifiable predictions

within the MESTR framework.

A22 Replication and Compliance Checklist

Conceptual integrity: EHI used only as an environmental constraint measure.

Spatial unit specified and consistent across components.

Temporal window stated (≥20–30 years recommended) and justified.

Solar irradiation included (or exclusion justified explicitly).

NPP included (or exclusion justified explicitly).

Cold extreme, seasonality, and photoperiodic hardship included.

Orientation verified: higher values indicate greater harshness for every component.

Scaling method (z-score or alternative) stated, including standardization domain.

Index formula and weights reported; any variant labeled EHI-X.

Missing data approach reported; sensitivity checks conducted.

Diagnostics provided: distributions, correlations, component dominance, leave-one-out index tests.

Interpretation discipline followed: non-normative, ecological-level, no circularity.

Code and data access provided (or fully reproducible pseudo-code).

Appendix B: Condensed Theoretical Foundation of MESTR

B1 Energetic Foundations of Selection

All adaptive systems operate under energetic constraint surfaces (Lotka, 1922; Odum, 1983; Smil 2004). Energy availability, capture efficiency, storage, and allocation jointly define the feasible space within which survival, reproduction, and complex trait formation can occur (Pontzer, 2016). From early thermodynamic perspectives on biological organization to later formulations in ecological energetics, a consistent principle emerge: selection acts not only on traits, but on the energetic viability of trait expression (Lotka, 1922; Odum, 1983; Smil, 2004).

Energy is not merely an environmental input; it is a constraint surface governing metabolic budgets across the annual cycle. Where usable energy is scarce, unpredictable, or seasonally compressed, organisms must allocate resources more strictly toward maintenance and survival. Under such conditions, both phenotypic variance and developmental latitude tend to narrow. Conversely, energetically permissive environments allow broader allocation, buffering, and diversification of trait expression.

The energetic foundation of MESTR therefore treats ecological constraint not as background noise but as a primary structuring force shaping selection regimes, variance distributions, and adaptive trade-offs.

B2 The MESTR Framework (Migration–Energy–Selection–Trait Redistribution)

MESTR formalizes the interaction between migration, ecological constraint, selection pressure, and trait distribution.

1 Migration redistributes populations across heterogeneous constraint landscapes, altering exposure to ecological pressures and reshaping variance structures through founder effects, filtering, and admixture.

2 Energy defines the ecological constraint field. Variation in usable energy and seasonal predictability imposes systematic pressures on survival strategies, developmental stability, and adaptive allocation.

3 Selection operates under these constraints. Environments that impose high energetic and temporal demands favor traits compatible with constraint management, while simultaneously narrowing admissible variance.

4 Trait Redistribution emerges downstream: population-level trait distributions reflect both historical migration paths and long-run ecological filtering, rather than immediate environmental conditions alone.

A central principle is exogeneity: ecological constraint must remain analytically separate from downstream traits and institutions. MESTR therefore treats environmental constraint as a conditioning field rather than an outcome.

B3 Environmental Constraint Surfaces

Ecological constraint is multidimensional and cannot be reduced to latitude or mean temperature alone. Several independent mechanisms shape energetic limitation and stress:

5 Incoming solar energy determines primary energetic input.
6 Net primary productivity reflects biologically captured energy.
7 Cold extremes impose thermoregulatory demands.
8 Thermal seasonality increases energetic coordination costs.
9 Photoperiodic variation constrains usable time and seasonal predictability.

Together these form a constraint surface that governs the temporal and energetic structure of adaptive systems. Different environments may exhibit similar overall constraint levels while differing in composition (e.g., cold-dominant vs low-energy vs photoperiodic regimes). Proper modeling therefore requires component-level analysis rather than single proxies.

B4 Variance Structure Under Constraint

A central prediction of the MESTR framework concerns variance regulation. Ecological constraint does not only shift mean outcomes; it shapes the range of viable variation.

Key mechanisms include:

10 Energetic filtering: high constraint reduces developmental latitude.
11 Temporal compression: shorter or harsher growth windows limit adaptive dispersion.
12 Serial founder effects: migration sequences reduce standing variation (Cavalli-Sforza, Menozzi, & Piazza, 1994)

13 Truncation selection under constraint further compresses variance.

Thus, increasing ecological harshness tends to reduce admissible variance in downstream traits even when mean changes are modest. This produces mean–variance decoupling, where variance shifts may exceed mean shifts in magnitude.

B5 Mean–Variance Law

Let ecological constraint be represented by long-run harshness level *EHI* and ecological heterogeneity by *Var(EHI)* within a domain. For a population-level outcome *Y*:

14 Mean constraint effect: E[Y] = f(EHI) (monotonic, potentially nonlinear)

15 Variance compression under constraint:

$$\frac{\partial \mathrm{Var}(Y)}{\partial \mathrm{Var}(EHI)} < 0.$$

16 Environmental variance amplification with latitude:

$$\frac{\partial \mathrm{Var}(EHI)}{\partial \mid \mathrm{Latitude} \mid} > 0,$$

17 Joint variance law:

$$\mathrm{Var}(Y) = \alpha - \beta_1 EHI - \beta_2 \mathrm{Var}(EHI), \text{ with } \beta_1, \beta_2 > 0$$

These relations are falsifiable and define the empirical test space of the framework.

B6 Migration–Selection Coupling

Migration interacts with ecological constraint in two principal ways:

18 Founder compression: serial migration reduces genetic and phenotypic variance.
19 Constraint filtering: ecological pressures differentially retain viable trait ranges.

Together they produce structured global variance gradients and regionally stable trait distributions shaped by both ecological and demographic history.

B7 Energetic Coordination Cost

Beyond energy scarcity, environments impose coordination demands: managing seasonal variability, storage, thermal regulation, and temporal synchronization. High variability environments require more precise allocation and buffering, increasing systemic coordination cost even where mean energy is not minimal. This mechanism contributes to variance compression and adaptive specialization.

B8 Position of EHI within MESTR

The Environmental Harshness Index operationalizes ecological constraint as a measurable, exogenous surface. EHI is not a trait, outcome, or normative

ranking; it is a constraint descriptor enabling comparative analysis across regions and periods.

Within MESTR:

20 EHI represents the ecological conditioning field.
21 Selection operates conditional on EHI.
22 Trait distributions emerge downstream.
23 EHI must remain analytically independent of outcomes.

B9 Testable Predictions

The framework yields falsifiable expectations:

24 Mean outcomes shift with long-run ecological constraint.
25 Outcome variance declines as ecological constraint increases.
26 Ecological variance increases with latitude.
27 Variance compression can occur without large mean shifts.
28 Failure of variance decline under high constraint challenges the framework.

B10 Scope and Limits

MESTR operates at ecological and population levels. It does not imply individual determinism. Institutional buffering and technological adaptation may modify outcomes but do not eliminate underlying constraint structures. Ecological inference limitations apply, and historical reconstructions introduce uncertainty that must be reported explicitly.

B11 Relation to Part I

This appendix provides only the minimal theoretical architecture required to interpret the Environmental Harshness Index and its predictions. The full theoretical development—including historical foundations, formal derivations, and extended argumentation—is presented in the first parts of this volume.

Appendix C: Formal Mean–Variance Derivation

Let ecological constraint E reduce feasible trait space through energetic filtering and truncation selection. Suppose baseline outcome variance without constraint is σ_0^2.

Energetic filtering reduces variance proportionally:

$\mathrm{Var}(Y \mid EHI) = \sigma_0^2 \cdot \exp(-kEHI)$

where $k > 0$ reflects constraint strength.

Ecological heterogeneity introduces additional compression:

$\mathrm{Var}(Y) = \sigma_0^2 \cdot \exp(-k_1 EHI - k_2 \mathrm{Var}(EHI))$

Linearizing for moderate EHI:

$\mathrm{Var}(Y) \approx \alpha - \beta_1 EHI - \beta_2 \mathrm{Var}(EHI)$

with $\beta_1, \beta_2 > 0$.

Thus:

$$\mathrm{Var}(Y) = \alpha - \beta_1 EHI - \beta_2 \mathrm{Var}(EHI), \beta_1, \beta_2 > 0,$$

which constitutes the joint variance law, also stated elsewhere.

The static variance law describes the equilibrium condition implied by the dynamic variance equation.

Empirical violation of these inequalities falsifies the constraint-variance prediction.

Appendix D: Mathematical Appendix; Formal EHI Construction

D1 Energetic Structure

Let:

1. P = Net primary productivity (normalized)
2. T_c = Cold stress index (derived from Tmin and temperature seasonality)
3. S_p = Photoperiod / seasonal constraint index

Define standardized variables:

$$P' = \frac{P - \mu_P}{\sigma_P}, T' = \frac{T_c - \mu_T}{\sigma_T}, S' = \frac{S_p - \mu_S}{\sigma_S}$$

Because low productivity increases harshness, invert productivity:

$$P_h = -P'$$

D2 Composite Harshness Function

$$EHI = w_1 P_h + w_2 T' + w_3 S'$$

where weights w_i may be equal or empirically estimated.

D3 Energetic Interpretation

Let ecological input:

$$E_{in} \propto P$$

Maintenance cost:

$$E_{maint} \propto f(T_c, S_p)$$

Then:

$$EHI \approx \frac{E_{maint}}{E_{in}}$$

D4 Optional Nonlinear Form

$$EHI = \log\left(\frac{E_{maint}}{E_{in}}\right)$$

which stabilizes variance and reflects proportional energetic constraint.

Appendix E: Variable and Equation Inventory

I. VARIABLES (complete list)

Core state variables

- V— variance in coordination-relevant traits x
- Y— outcome variable (e.g., institutional performance)
- $\mathrm{Var}(Y)$— outcome variance
- I— institutional stability

Environmental / constraint variables

- EHI— Environmental Harshness Index (ecological/thermodynamic constraint)
- T— technological buffering

Dynamic / structural parameters

- t— generational time
- α— strength of variance compression (selection intensity)
- β— strength of variance expansion (buffering effect)
- K— upper bound (carrying capacity for variance)

Trait-level variables

- x— coordination-relevant trait
- $f(x)$— distribution of trait x
- x_c— viability threshold

- $W(x)$— fitness function

Founder effect variables

- V_0— ancestral variance
- V_k— variance after $k$migration steps
- f_i— fraction of variance lost at step i
- k— number of migration steps

Energy allocation variables (Section 3.7)

- E_{total}— total metabolically usable energy
- E_{in}— energy input
- $E_{surplus}$— net available energy
- E_{maint}— maintenance energy
- E_{growth}— growth energy
- E_{repro}— reproductive energy
- E_{neural}— neural/cognitive energy
- E_{buffer}— storage/buffering energy

II. EQUATIONS (master set)

1. Institutional stability

$$I \propto \frac{1}{V}$$

2. Selection gradient

$$S \propto (EHI - T)$$

3. Core variance dynamics equation

$$\frac{dV}{dt} = -\alpha(EHI - T)\,V + \beta T\left(1 - \frac{V}{K}\right)$$

4. Founder effects (multiplicative variance loss)

$$V_k = V_0 \prod_{i=1}^{k} (1 - f_i)$$

5. Truncation selection (fitness function)

$$W(x) = \begin{cases} 1 & \text{if } x \geq x_c \\ 0 & \text{if } x < x_c \end{cases}$$

6. Threshold dependence on constraint

$$x_c = x_c(EHI)$$

$$\frac{\partial x_c}{\partial EHI} > 0$$

$$x_c \propto (EHI - T)$$

7. Variance update under truncation

$$V(t+1) = \mathrm{Var}(x \mid x \geq x_c)$$

$$V(t+1) < V(t)$$

8. Mean constraint prediction

$$\mathbb{E}[Y] = f(EHI), f'(EHI) \neq 0$$

9. Variance amplification (environmental)

$$\frac{\partial \mathrm{Var}(EHI)}{\partial \mid Latitude \mid} > 0$$

10. Variance inversion (outcomes)

$$\frac{\partial \mathrm{Var}(Y)}{\partial \mathrm{Var}(EHI)} < 0$$

11. Joint variance model

$$\mathrm{Var}(Y) = \alpha - \beta_1 EHI - \beta_2 \mathrm{Var}(EHI), \beta_1, \beta_2 > 0$$

12. Energy conservation identity (micro-foundation)

$$E_{total} = E_{maint} + E_{growth} + E_{repro} + E_{neural} + E_{buffer}$$

13. Surplus energy constraint

$$E_{surplus} = E_{in} - E_{maint}$$

14. Selection gradient (relinked to energy)

$$S \propto (EHI - T)$$

(reappears as bridge between energy allocation and variance dynamics)

15. Full integrated system (implicit synthesis)

Combining energy and variance:

$$EHI \uparrow \Rightarrow E_{maint} \uparrow \Rightarrow E_{surplus} \downarrow \Rightarrow V \downarrow$$
$$T \uparrow \Rightarrow E_{surplus} \uparrow \Rightarrow V \uparrow$$

Author index

References

Aiello, L. C., & Wheeler, P. (1995). The expensive-tissue hypothesis: The brain and the digestive system in human and primate evolution. *Current Anthropology, 36*(2), 199–221.

Akbari, A., Barton, A. R., Gazal, S., Li, Z., Kariminejad, M., Perry, A., Zeng, Y., Mittnik, A., Patterson, N., Mah, M., Zhou, X., Price, A. L., Lander, E. S., Pinhasi, R., Rohland, N., Mallick, S., & Reich, D. (2024). Pervasive findings of directional selection realize the promise of ancient DNA to elucidate human adaptation. *bioRxiv*. https://doi.org/10.1101/2024.09.14.613021

Anthony, D. W. (2007). *The horse, the wheel, and language: How Bronze-Age riders from the Eurasian steppes shaped the modern world*. Princeton University Press.

Beals, K. L., Smith, C. L., & Dodd, S. M. (1984*).* Brain size, cranial capacity, and allometry: A re-assessment. *Human Biology, 56*(2), 213–235.

Becker, D. (2019). National IQ (NIQ) data set (Version 1.3.3) [Data set]. *Open Science Framework*. https://osf.io/

Biasutti, R. (1967). *Le razze e i popoli della terra (4th ed.).* Torino, Italy: Unione Tipografico-Editrice Torinese (UTET).

Boltzmann, L. (1886/1974). *The second law of thermodynamics*. In S. G. Brush (Ed. & Trans.), Theoretical physics and philosophical problems: Selected writings (pp. 13–32). Dordrecht, Netherlands: Reidel. (Original lecture delivered 29 May 1886 at the Festive Session of the Imperial Academy of Sciences in Vienna).

Brown, J. H., Gillooly, J. F., Allen, A. P., Savage, V. M., & West, G. B. (2004). Toward a metabolic theory of ecology. *Ecology, 85*(7), 1771–1789.

Cavalli-Sforza, L. L., Menozzi, P., & Piazza, A. (1994). *The history and geography of human genes*. Princeton University Press.

Central Intelligence Agency. (2022). *The World Factbook*: Mother's mean age at first birth [Data set]. Central Intelligence Agency.

CEPII. (2011). GeoDist database. Centre d'Études Prospectives et

d'Informations Internationales, Paris.

https://www.cepii.fr/CEPII/en/bdd_modele/bdd_modele_item.asp?id=6.

Cherson, A. D. (2012). *Atlas of Genetic Genealogy*. Greencore Environmental Information Services. Retrieved from http://atlas.xyvy.info.

Clarke, A., & Fraser, K. P. P. (2004). Why does metabolism scale with temperature? *Functional Ecology, 18*(2), 243–251.

Darwin, C. (1859/1872). *On the origin of species by means of*

natural selection. John Murray.

Danish Finance Ministry (2021): https://www.economist.com/sites/

default/files/image/print-edition/20211218_EUC232.png?utm_

source=substack&utm_medium=email.

Economist Intelligence Unit. (2024). *Democracy Index 2023: Age of conflict*. The Economist Intelligence Unit.

Ellis, B. J., Figueredo, A. J., Brumbach, B. H., & Schlomer, G. L. (2009). Fundamental dimensions of environmental risk: The impact of harsh versus unpredictable environments on the evolution and development of life-history strategies. *Human Nature, 20*(2), 204–268. https://doi.org/10.1007/s12110-009-9063-7

Ellis, L., Hoskin, A. W., & Buker, N. H. (2021). National variations in CAG repeats of men's androgen receptor gene: A tabulated review. *Mankind Quarterly, 61*(3), 430–461.

Falconer, D. S., & Mackay, T. F. C. (1996). *Introduction to quantitative genetics* (4th ed.). Longman.

Fick, S. E., & Hijmans, R. J. (2017). WorldClim 2: New 1-km spatial resolution climate surfaces for global land areas. *International Journal of Climatology*, *37*(12), 4302–4315.

https://doi.org/10.1002/joc.5086.

Fisher, R. A. (1930). *The genetical theory of natural selection*. Clarendon Press.

Forsythe, W. C., Rykiel, E. J., Stahl, R. S., Wu, H., & Schoolfield, R. M. (1995). A model comparison for daylength as a function of latitude and day of year. *Ecological Modelling, 80*(1), 87–95.

Gibney, M., Cornett, L., Wood, R. M., Haschke, P., & Arnon, D. (2024). *The Political Terror Scale 1976–2023* [Data set]. Political Terror Scale Project.

Galor, Oded. (2011). *Unified Growth Theory*. Princeton University Press, Princeton NJ,; ISBN 978-0-691-13802-2 · DOI 10.1515/9781400838863.

Galor, Oded. (2022). *The Journey of Humanity: The Origins of Wealth and Inequality*. Dutton, New York; ISBN 978-0-593-18804-0

Helliwell, J. F., Layard, R., & Sachs, J. (Eds.). (2015). *World Happiness Report 2015*. New York, NY: Sustainable Development Solutions Network.

Institute for Economics & Peace. (2017). *Global Peace Index 2017: Measuring peace in a complex world*. Institute for Economics & Peace.

Jensen, A. R. (1998). *The g factor: The science of mental ability*. Praeger. (Spearman, 1927; Jensen, 1998)

Jensen, S., & Kirkegaard, E. O. W. (2024). *National IQs and socioeconomic development.* (OSF Preprint). https://doi.org/10.31234/osf.io/bx86g. (Provides the updated cross-national cognitive ability measure used in the present study).

Kaplan, H., Hill, K., Lancaster, J., & Hurtado, A. M. (2000). A theory of human life history evolution: Diet, intelligence, and longevity. *Evolutionary Anthropology, 9*(4), 156–185.

Kuzawa, C. W., Chugani, H. T., Grossman, L. I., Lipovich, L., Muzik, O., Hof, P. R., Wildman, D. E., Sherwood, C. C., Leonard, W. R., & Lange, N. (2014). Metabolic costs and evolutionary implications of human brain development. *Proceedings of the National Academy of Sciences, 111*(36), 13010–13015.

Lazaridis, I., Patterson, N., Anthony, D. W., Vyazov, L., Fournier, R., Ringbauer, H., Olalde, I., Khokhlov, A. A., Kitov, E. P., et al. (2025). The genetic origin of the Indo-Europeans. *Nature, 639*, 132–142.

Lim, S. S., Updike, R. L., Kaldjian, A. S., Barber, R. M., Cowling, K., York, H., et al. (2018). Measuring human capital: A systematic analysis of 195 countries and territories, 1990–2016. *The Lancet, 392*(10154), 1217–1234.

Lotka, A. J. (1922). Contribution to the energetics of evolution. *Proceedings of the National Academy of Sciences, 8*(6), 147–151.

Maynard Smith, J. (1989). *Evolutionary genetics*. Oxford University Press. (on truncation selection and robustness).

Meisenberg, G. (2015). Are cognitive differences between countries diminishing? Evidence from TIMSS and PISA. *Intelligence, 48*, 149–157.

Murray, C. (2003). *Human Accomplishment: The pursuit of excellence in the Arts and Sciences 800 B.C. to 1950*. New York: Harper-Collins Publishers.

NASA Earth Observatory. (2023). *Energy balance and the Earth's climate*. NASA. https://earthobservatory.nasa.gov/features/EnergyBalance/page2.php

NASA Earth Observatory. (2023). *Earth's energy budget and climate*. NASA. National Academy of Sciences, 8(6), 147–151.

https://doi.org/10.1073/pnas.8.6.147.

NCD Risk Factor Collaboration (NCD-RisC). (2016). *A century of trends in adult human height.* eLife, 5, e13410.

NCD Risk Factor Collaboration (NCD-RisC). (2017). Worldwide trends in body-mass index, underweight, overweight, and obesity from 1975 to 2016: A pooled analysis of 2416 population-based measurement studies in 128.9 million children, adolescents, and adults. *The Lancet, 390*(10113), 2627–2642.

Nyborg, H. (1994). *Hormones, sex, and society: The science of physicology*. Westport, CT: Praeger. (downloadable from www.helmuthnyborg,dk).

Nyborg, H. (1997). Molecular man in a molecular world: Applied physicology. *Psyke & Logos, 18,* 457–474. (downloadable from www.helmuthnyborg.dk.

Odum, H. T. (1983). *Systems ecology: An introduction*. Wiley.

Odum, H. T. (1995a*). Environmental accounting: Emergy and environmental decision making*. Wiley.

Odum, H. T. (1995b). *Self-organization and maximum power*. University Press of Colorado.

Pontzer, H. (2017). The crown joules: energetics, ecology, and evolution in humans and other primates. *Evolutionary Anthropology, vol. 26,* Issue 1, 12-23.

Pontzer, H. (2017). *The energetics of human evolution*. Princeton University Press.

Pontzer, H. (2017). *Burn: New research blows the lid off how we really burn calories*. Penguin.

Pontzer, H. (2021). *Burn: The misunderstood science of metabolism*. New York: Penguin.

Pontzer, H., & Raichlen, D. A. (2021). Energetic allocation and trade-offs in primate life histories. *Scientific Reports, 11*(1), 93764. https://doi.org/10.1038/s41598-021-93764-x

Pontzer, H., Brown, M.H., Raichlen, D.A., Dunsworth, H., Hare, B., Walker, K., Luke, A., Dugas, L.R., Durazo-Arvizu, R., Schoeller, D.A, Plange-Rhule, J., Bovet, R., Forrester, T.E., Lambert, E.V., Thompson, M.E., Shumaker, R.W., & Ross, S.R. (2016). Metabolic acceleration and the evolution of human brain size and life history. *Nature, 533*, 390– 392.

Prigogine, I., & Stengers, I. (1984). *Order out of chaos: Man's new dialogue with nature*. Bantam.

Rindermann, H. (2007). The *g*-factor of international cognitive ability comparisons: The homogeneity of results in PISA, TIMSS, PIRLS and IQ tests across nations. *European Journal of Personality, 21*(5), 667–706.

Rindermann, H. (2018). *Cognitive capitalism: Human capital and the wellbeing of nations.* Cambridge University Press. (Provides updated cross-national cognitive ability measures, including student-assessment composites used in this study).

Rindermann, H., & Becker, D. (2016). National cognitive ability, human capital, and economic growth: A review update. *Journal of Intelligence, 4*(1), 20.

Rindermann, H., Woodley of Menie, M. A., & Stratford, J. (2012).

Haplogroups as Evolutionary markers of cognitive ability.

Intelligence, 40(4), 362–375.

https://doi.org/10.1016/j.intell.2012.04.002.

Running, S. W., Nemani, R. R., Heinsch, F. A., Zhao, M., Reeves,

M., & Hashimoto, H. (2004). A continuous satellite-derived measure of global terrestrial primary production. *BioScience, 54*(6), 547–560.

https://doi.org/10.1641/0006-568(2004)054[0547: ACSMOG]2.0.CO;2

Schrödinger, E. (1944). *What is life? The physical aspect of the*

living cell. Cambridge University Press.

Schuster, P. (2007). Boltzmann and evolution: Some basic questions of biology seen with atomistic glasses. In P. M. Binder, H. L. Frisch, & W. P. Reinhardt (Eds.), *Physical biology: From atoms to medicine* (pp. 3–24). Springer. https://doi.org/10.1007/978-3-540-45612-8_1.

Smil, V. (2004). *Energy in world history*. Westview Press.

Spearman, C. (1904). General intelligence, objectively determined

and measured. *The American Journal of Psychology, 15*(2), 201-292.

https://doi.org/10.2307/1412107.

Spearman, C. (1927). *The abilities of man*. Macmillan.

Spolaore, E., & Wacziarg, R. (2009). The diffusion of development. *Quarterly Journal of Economics, 124*(2), 469–529.

Stearns, S. C. (1992). *The evolution of life histories*. Oxford University Press.

The Economist Intelligence Unit. (2023). *Democracy Index 2023*. EIU.

The Fund for Peace. (2023). *Fragile States Index 2023: Annual report*. Washington, DC: The Fund for Peace.

Transparency International. (2024). *Corruption Perceptions Index 2023: Defying democracy.* Transparency International.

United Nations Development Programme. (2022). *Human Development Report 2021/2022: Uncertain times, unsettled lives*. UNDP.

United Nations Development Programme. (2023). *Education index 2023* [Data set]. UNDP Human Development Data Center.

United Nations Development Programme. (2024). *Human Development Index and its components, 2023 (HDI values and ranks for 193 countries and territories)* [Data set]. In Human Development Data Center. UNDP. (Original data in HDR 2025 Statistical Annex, Table 1 “Human Development Index and its components.

UNODC. (2019). United Nations Office on Drugs and Crime. *Global Study on Homicide 2019*.

Vanhanen, T. (2012). *Ethnic conflicts: Their biological roots in ethnic nepotism*. London, UK: Ulster Institute for Social Research.

Waddington, C. H. (1957). *The strategy of the genes*. Allen & Unwin. (on canalization).

West, G. B., Brown, J. H., & Enquist, B. J. (1997). A general model for metabolic scaling laws in biology. *Science, 276*(5309), 122–126.

World Bank. (2024a). *World Development Indicators: Scientific and technical journal articles (per 1,000 people), 2017* [Data set]. World Bank

World Bank. (2024b). *Poverty and Inequality Platform (PIP): Gini index (World Bank estimate), 2017, by country and territory* [Data set]. World Bank.

World Bank. (2024c). *World Development Indicators: Intentional homicides (per 100,000 people), 2017* [Data set]. World Bank. (Data primarily from UN Office on Drugs and Crime and WHO).

World Bank. (2024d). *World Development Indicators: Road traffic injury death rate (per 100,000 people), 2017* [Data set]. World Bank.

World Health Organization. (n.d.). *UV radiation*. Global Health Observatory Data Repository. https://www.who.int/data/gho/data/indicators/indicator-details/GHO/uv-radiation

World Health Organization. (2018). *Global status report on road safety 2018*. World Health Organization.

World Health Organization. (2019). Solar ultraviolet (UV) radiation exposure: Population-weighted ambient UVR (1997–2003) [Indicator metadata and dataset].

Conceptual Contributions
Human populations evolved under widely different ecological conditions. From energy-rich equatorial environments to cold and highly seasonal northern regions, environmental constraints impose systematic energetic demands on survival, cooperation, and social organization.
This book introduces the Environmental Harshness Index (EHI) and the MESTR framework (Migration-Energetic Selection and Trade-offs), linking planetary energy flows to evolutionary outcomes in human populations.
Drawing on climatology, ecological energetics, and evolutionary theory, the framework proposes that long-term environmental harshness shapes the energetic costs of coordination, planning, and cooperation.
Where environments impose stronger energetic constraints—through cold climates, high seasonality, or reduced biological productivity—selection pressures may favor traits that enhance coordination efficiency and long-term planning.
By integrating thermodynamics, ecology, and global environmental data, the book proposes a unified perspective on how planetary energy gradients influence the evolution of intelligence and civilization.
Introduces the Environmental Harshness Index (EHI) as a quantitative measure of ecological constraint.
Develops the MESTR framework (Migration-Energetic Selection and Trade-offs) linking energy flows to evolutionary outcomes.
Integrates thermodynamics, ecology, and evolutionary theory into a unified explanatory model.
Demonstrates how planetary energy gradients shape coordination demands and social complexity.
Proposes a new perspective on the energetic foundations of intelligence and civilization in anatomically modern humans.
KASANDROBOOKS
MONOGRAPHS
ISBN 978-87-975315-2-6
9 788797 525126
KASANDROBOOKS MONOGRAPHS IN HUMAN ENERGETICS
The Evolution of Intelligence and Civilization
How Thermodynamic Constraints Shape Minds, Societies, and History
Solar Energy
Thermodynamic Constraints
Variance Dynamics
Coordination Demands and Trade-offs
Cognitive Adaptations
Civilization
Technology
$EHI = w_1 \Delta T + w_2 |T_{amp}| + w_3 \sigma_p + w_4 (1 - NPP) + w_5 D_s$
Helmuth Nyborg
KASANDROBOOKS
The Evolution of Intelligence and Civilization
Helmuth Nyborg
About the Author
Helmuth Nyborg
Born 1937 in Løsning, Denmark.
Professor Emeritus of Child and Developmental Psychology.
Aarhus University, Denmark (1968–2007).
Dr. phil., mag. art.
www.helmuthnyborg.dk
kasandrobooks.com